A Hybrid Approach for Lungs Nodule Detection using Deformable Model and Distance Transform

Babar Jehangir

686-FBAS/MSCS/F12

Department of Computer Science & Software Engineering

Faculty of Basic and Applied Sciences

International Islamic University Islamabad

2016

MS Thesis

A Hybrid Approach for Lungs Nodule Detection using Deformable Model and Distance Transform

Submitted in partial fulfillment of the requirements for the
MS Degree in Computer Science in Computer Sciences & Software Engineering Department

Supervisor:
DrAyyaz Hussain
Assistant Professor, at the Department of
Computer Science & Software Engineering,
International Islamic University Islamabad,
Pakistan

Babar Jehangir
686-FBAS/MSCS/F12

Department of Computer Science & Software Engineering
Faculty of Basic and Applied Sciences
International Islamic University Islamabad
2016

رَبِّ زِدْنِیْ عِلْمًا ۞

(طٰہٰ: 114)

اے میرے رب! میرے علم میں اضافہ فرما۔

In the name of
Allah,
The most Merciful and Compassionate the most Gracious and the Beneficent whose help and Guidance we always solicit at every step, and every moment.

Date: 21st March, 2016

Final Approval

This is to certify that we have read and evaluated the thesis titled **"A Hybrid Approach for Lungs Nodule Detection using Deformable Model and Distance Transform"** submitted by **Babar Jehangir** under **Reg No.686-FBAS/MSCS/F12.** It is our judgment that this thesis is of sufficient standard to warrant its acceptance by International Islamic University, Islamabad for the degree of MS in Computer Science.

VIVA VOICE COMMITTEE

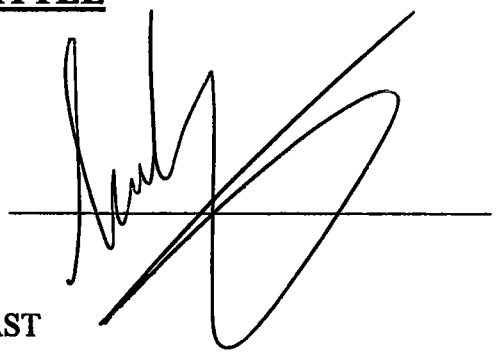

External Examiner
Dr. HASSAN MUJTABA
Associate Professor,
Department of Computer Science
National University of Computer &Emerging Sciences- FAST
Islamabad

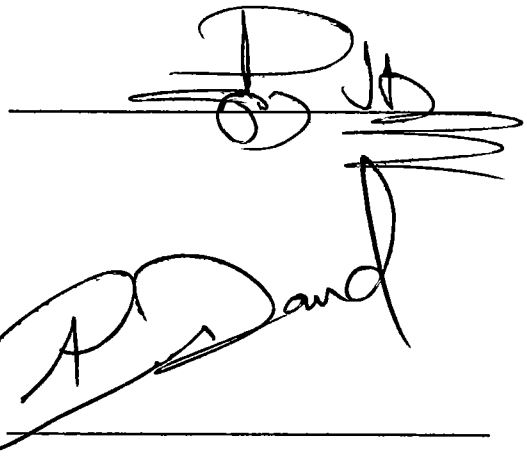

Supervisor
Dr. AYYAZ HUSSAIN
Assistant Professor,
Department of Computer Science & Software Engineering,
International Islamic University, Islamabad.

Internal Examiner
Dr. ALI DAUD
Assistant Professor,
Department of Computer Science & Software Engineering,
International Islamic University, Islamabad

Dedication

I dedicate this project to Allah, Hazrat Muhammad (PBUH), my beloved family, respected teachers and all those who helped and prayed for my success. Last but not least this dissertation is dedicated to my late father who has been my constant source of inspiration, Papa this is for you.

DECLARATION

I **BABAR JEHANGIR S/O MUHAMMAD AZRAM**
Registration No. **686-FBAS/MSCS/F12**

Student of MS in Computer Science at International Islamic University do hereby solemnly declared that the thesis entitled **"A Hybrid Approach for Lungs Nodule Detection using Deformable Model and Distance Transform"**, submitted by me in partial fulfillment of MS degree in Computer Science, is my original work, except where otherwise acknowledgement in the text, and has been submitted or published earlier and shall not, in future, be submitted by me for obtaining any degree from this or any other university or institution.

Student's Signature
Date: 21st March, 2016.

DECLARATION

I Prof/Dr AYYAZ HUSSAIN
Supervisor of student Mr. BABAR JEHANGIR

do hereby solemnly declare that the thesis entitled **"A Hybrid Approach for Lungs Nodule Detection using Deformable Model and Distance Transform"**, being submitted as partial fulfillment of MS degree in the discipline of **Computer Science** has been completed under my guidance and supervision and is an original work of the student except where otherwise acknowledged in the text. It has not been submitted or published earlier for obtaining any degree from this or any other university or institution.

This thesis is completed in all aspects and I am fully satisfied with the quality of student's research work. Now it is ready to be evaluated by external subject experts.

Date: 21st March, 2016

Name in full: Dr. AYYAZ HUSSAIN
Address: Assistant Professor, at the Department Of Computer Science & Software Engineering, International Islamic University Islamabad, Pakistan.
Email: ayyaz.hussain@iiu.edu.pk

Signature: 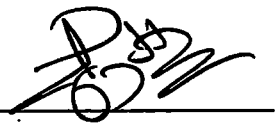

Acknowledgment

I wish to express my sincere gratitude to my guide, assistant professor Dr. Ayyaz Hussain, for his guidance, support and encouragement during my study of master of computer science at the Department of Computer Science and Software Engineering, International Islamic University, Islamabad, Pakistan. I am particularly indented to him for teaching me the research and writing, which proved beneficial to my current research and future career. Without his support, efforts, knowledge, patience and answers to my many questions, this research would not have been possible. Experimental methods and results presented in the thesis have been influenced by him in one way to another. It was a great honor and pleasure for me to do research under his guidance and supervision. I would like to thank all the members of the Department of Computer Science and Software Engineering, who helped me by providing the necessary resources, and in the various ways, in the completion of my work.

My deepest gratitude to my family who are the real pillars of my life. They always encouraged me and showed their everlasting love, care and support throughout my life. Their continuous encouragement and , humble prayers, support (both financial and moral) from my mother and my wife is unforgettable. I am also thankful to brothers SohailAzram and Muhammad Yasir for their love, care and support in my life.

I am also thankful to all my friends for their emotional support, entertainment, love and care they provided.

I want to dedicate this thesis to my parents. In one sentence, they meant everything to me.

Babar Jehangir

ABSTRACT

Hybrid approach for lungs nodule detection using deformable model and distance transform is a CAD scheme which detected all major kinds of nodules like juxtaplueral, isolated, juxtavescular and non-solid nodules. This CAD schemes has four major steps: In first step lungs segmentation has been performed using linear interpolation and lungs parenchymal volume identification in lungs parenchymal volume identifications there are two further processes are involved which are known as inclusion process and connectivity analysis. In third step of this CAD scheme nodule candidates were detected using deformable model and distance transform, due to complex structure of juxtavescular nodules distance transform is separately applied to detected juxtavescular nodules. In the fourth and last step rule based pruning is performed to remove false positives. Results of this CAD scheme is 95.2 % sensitivity with 4.85 false positives per scan and detected various sizes of nodules from 3mm to 30mm. This CAD scheme is tested on Lungs Image Database Consortium (LIDC) publically available database, in which there is 84 patients data and four radiologists give their results on it. As we know that to diagnose lungs cancer at earlier stages increases survival rate so this CAD scheme helps the physicians to detect lungs nodule on earlier stages.

TABLE OF CONTENTS

7 References

Chapter 1
Introduction

1.1 Introduction:

Around the globe lungs cancer is one of the most dangerous cancer. As per medical reports lungs cancer is the most frequent reason of death among the all types of cancers [1, 2]. Among the cancers, lung cancer has second lowest survival rate followed by pancreas cancer in the five year relative survival (Figure 1.1).The survival rates are less than 10% both male and female [3].Recent reports about lungs cancer indicates that continued existence rate of lung cancer in most recent five years is varying between 13% to 21% this rate is increases up to 50% if lungs nodules are detected on early stages. Nearly 70% lungs cancer detection at early stages effects the treatment. As per statistics taken from 2008 which shows lung cancer is a viral disease which attacks the greater number of people in the whole world. As per last global estimate that indicates the happening of 1,200,000 new cases of the lungs infection 2000 [4]. Among all different types of cancers lungs cancer have larger occurrence rate and one of the highest death rate. Regrettably, in the era of latest technologies still determination is regularly made late, which affects treatment results. Diagnosing lung cancer using low dose computed tomography is a big hope for changing this situation in accomplishing a more intelligent conclusion of lung tumor.

Two main reasons in the lungs cancer, first of all it is very difficult to diagnose it at early stages due to insufficiency of symptoms and second is the poor prognostics when the infection is detected at more near the beginning phase. However, it is hard to diagnose early that pulmonary nodule exist or not, and this nodule is malignancy or not, because the diagnosis system is not efficient. When radiologists diagnose one of the patients, they need to analyze with respect to hundreds of the Computed Tomography (CT) images with the naked eye. This existing system can be easy to mistake the diagnosis. For this reason, Computer Aided Diagnosis (CAD) system is studied largely [9-10]. There are many researchers who works and investigate on CAD to improve their accuracy level.

CAD – computer-aided diagnosis has been based on finding made by radiologists who explained the computer output based on quantitative analysis of radiological images. The basic idea/steps used in CAD schemes are first one is processing of images for extraction and detection of nodule candidates from the images, second one is image feature's quantitation for candidates of abnormalities and the third one is classification of data which differentiate between abnormal and normal features of lungs images (or benign and malignant) and the fourth and last one is

quantitative assessment and recovery of pictures like those of obscure sores. In lungs tumor computer tomography (CT) is a standout amongst the most responsive method of detecting lungs nodule. A figured tomography (CT) sweep is an imaging technique that uses X-beams to make pictures of cross area of the body. Automated nodule recognition plans have been appeared to significantly increment indicative precision in radiological imaging [5, 6].

An important point which needs to be considered that the radiologist analysis is mainly based on the morphological structures under investigation which can be checked in 3D space and the examination of a CT is performed through bi-dimensional pictures that's why tradeoff between the radiologists needs to watch and what is appeared to him requires a remaking of the tri-dimensional parts of the tissue under investigation undertaking which other than intricate and moderate and during this reconstruction process lots of chances for mistakes. That's the major reason in greater demand of computational frameworks which can help with the undertakings of discovery and analysis of lung nodules and therefore number of published paper increases every year in this field. [7].

To detect nodule in the lungs we are going to introduce a computer-aided diagnosis (CAD) system which helps the radiologists to detect nodule from the lungs in faster, accurate and efficient manner. There is four main tasks involve in this the CAD system, these are as follows: 1) Initial selection of nodule list 2) Lung nodule segmentation 3) Lungs nodule detection and 3) Classification of detected nodules. CAD system, we are going to introduce will detect from small size of nodule (3mm) to very large size of nodule (30mm).Another salient and distinguish contribution of this CAD scheme is; it not focus on only a single type of nodules it has the ability to detect all kind of nodules like isolated, juxtapleural and juxtavescular nodules. Larger size of juxtavescular nodules are difficult to detect due to their complex structure but this scheme will detect larger size of juxtavescular nodules.

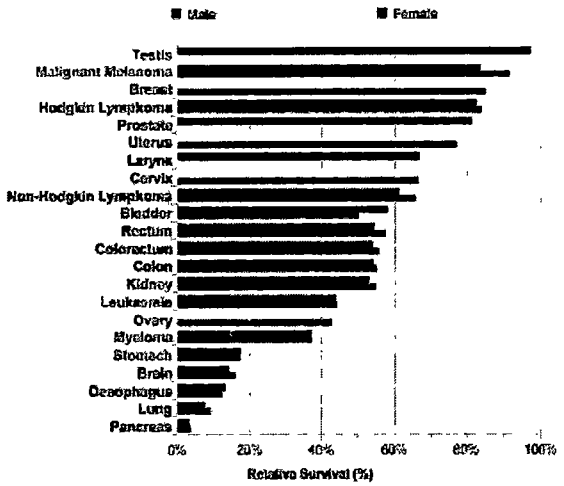

Figure 1.1: Five Year Age Standardized relative survival for adults (aged 15-99years); diagnosed during 2005 2009 and followed up to 2010: England, 21 common cancers, by Sex.

1.2 Problem Domain

All around the globe lots of researcher are working to find the ways to detect lungs cancer to detect it at early stages so that survival rate of lungs cancer can be increased upto 70% as we described in earlier section. Latest technologies were adopted to make the detection/ diagnosis procedure of lungs cancer more accurate and efficient. In this era many government agencies and as well private agencies spend lots of money and time to make a better diagnosis system. There are many cancer research centers all around the globe which work on generic cancer research along with territorial components. Computational systems are a fundamental part of all exploration endeavors on tumor. As discussed in previous section that survival rate of lungs cancer will be increased if it diagnosed at early stages. Below figure shows continued existence rate of early stage vs late stage diagnosis of last five years[8].

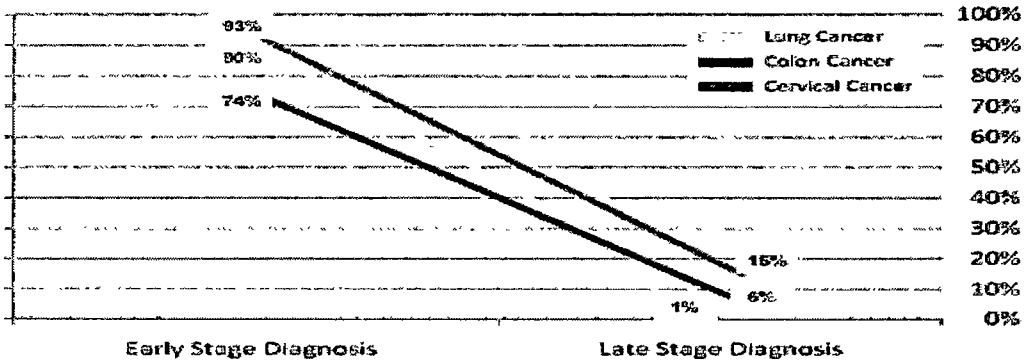

Figure 1.2: Five year relative survival: early stage vs. late stage diagnosis [8]

To diagnose lungs cancer at early stages Computer Aided Diagnosis system helps radiologists. Lots of CAD scheme were introduced by the researchers but still there is lots of work to do in this area. CAD scheme detect lung nodules from DICOM images. There is three main types of lungs nodule: i) Isolated Nodules ii) Juxtapleural Nodules iii) Juxtavescular Nodules. Isolated nodule neither attached with lungs wall nor with any voxel or any other structure of lungs it is fully isolated in lungs and easier to detect. Juxtapleural nodules are attached with lungs wall and its little bit difficult to detect as compared with isolated nodules. Juxtavescular nodules are those nodules which are attached with voxels and other structure of lungs, detection of these nodules are most difficult as compared to isolated and juxtapleural nodule.

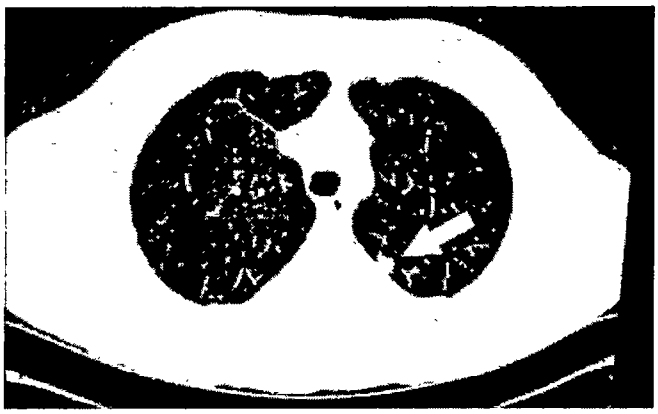

Figure1.3: Juxtapleural Nodules

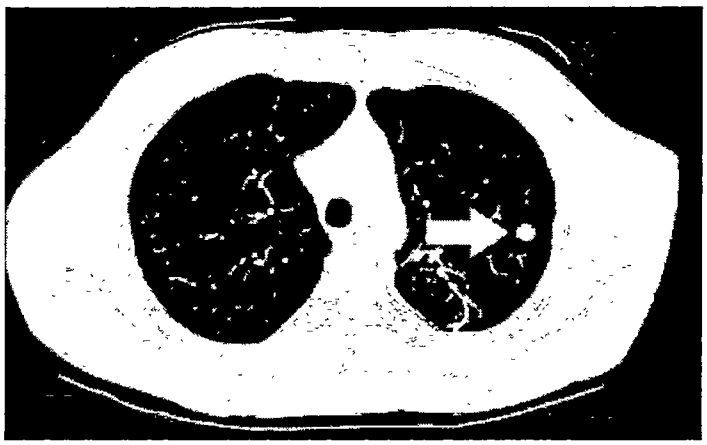

Figure 1.4: Isolated Nodules

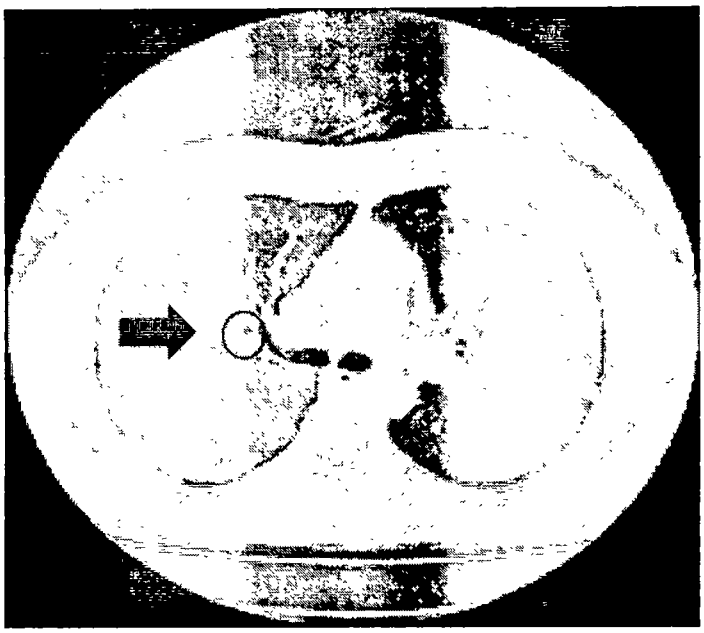

Figure 1.5: Juxtavescular Nodules

All these nodules have sizes from 3mm to 30mm. To detect all three types of nodules of all sizes is tough job. So there is a need to introduce a CAD scheme which detect all types and sizes of nodules. Which will play an important role to diagnose lungs cancer at early stages which will increase survival rate. So in this research we are going to introduce a CAD scheme which will detect all of types and sizes nodules. For last few decades image analysis techniques have been to analyze microscopic images, X-ray scans and CT scans. In our work we concentrate on macro scale imaging. The declaration of the imaging system enables tissue-level examination.

1.3 Research Objectives

The objective of this research is to build a CAD system which helps the radiologists to diagnose lungs cancer at early stages which increase the survival rate of lungs cancer. Complex structure in chest including mediastinum pulmonary vessels and ribs make it very difficult to detect lungs nodule at earlier stages when nodules are small and less visible.

This CAD system highlights abnormality that may be unnoticed by the physicians on starting stage of search.

The specialty of this CAD system is that it will detect all kinds of nodule from 3mm to 30mm.

- Determine the isolated, juxtavescular and juxtapleural nodules from complex structure of lungs.

- Reduce number of false positives using rule based pruning.

Ultimately our study will developed a CAD scheme which determine that whether the CAD schemes should be used or not for lungs nodule detection in diagnosis of lungs cancer.

1.4 Research Contributions

This thesis contributes to the region of pure investigational computer science. Specially, it develops a CAD scheme which helps the radiologists for lung cancer detection at early stages which increases the survival rate of the death of lung cancer. We have been building up a PC helped symptomatic (CAD) plan to help radiologists in enhancing the recognition of aspiratory knobs in lungs, because radiologists can miss as many as 30% of pulmonary nodules in routine clinical practice. Our major concern is to develop such CAD scheme in which very small number of flase positive which was falsely reported as nodule candidate by the CAD schemes and very high number of true positive (actual nodule candidates). In order to considerably reduce the number of false positives in our CAD scheme, we developed, in this study, a hybrid nodule detection technique, in which mainly all three types of nodule can be detected.

1.5 Research Methodology

1.5.1 Data Sets:

For this research study two publically available databases will be used. These are as follows:

1) *Database A:*The first database that will be used in our research work is Lung Image Database Consortium image collection (LIDC-IDRI), which consists of 1,010 lung malignancy screening thoracic CT examines with set apart up commented on sores. This database is publically available on the internet for development, training and evolution of computer aided detection (CAD) schemes for lung cancer detection and diagnosis.

2) *Database B:* Another publically online available database by collaboration between the Early Lung Cancer Action Program (ELCAP) and Vision and Image Analysis (VIA) research groups. The database consists of 50 low-dose whole-lung CT scans for detection. The truth table of nodules candidate is also provided by the radiologist.

1.5.2 Performance Measures:

Sensitivity of our CAD scheme to true nodule candidates can be found by separating total number of true positive by the total number of scans.

No. of True Positive Detections = TruePostives / totalnumber

The average number of false positives in our proposed CAD scheme can be found using following equation:

Average Number of False Positives = FP / m

'FP' represents the total false positive detections and 'm' is the number of scans.

Additionally, measures of precision and recall are calculated to evaluate system performance.

Precision is the division of recovered instances that are applicable and is known by:

Precision = TP / (TP + FP)

where 'TP' is the positive result for a nodule that exists, and 'FP' is a positive result for a nodule that does not exist.

Review is the part of significant occurrences that are recovered and is given by:

Review = TP / (TP + FN)

where 'TP' is the positive result for a nodule that exists, and 'FN' is a negative result for a nodule that exists.

1.6 Thesis Layout

Our thesis is based on six chapters. **Chapter 1** gives introduction to the topic along with discussion on problem domain, research objectives, research contribution and research methodology. **Chapter 2** gives comprehensive reviews on relevant literature about lungs nodule detection CAD schemes to help radiologists to detect lungs cancer at early stages to increase survival rate of lungs cancer. **Chapter 3** describes the problem statement which we have solved in this research. **Chapter 4** discuss as in detail the deformable model and distance transform to detect different types of lungs pulmonary nodules along with rule based pruning for false positive reduction. **Chapter 5** is about the results of CAD schemed we developed in this research study. In the last chapter which is **Chapter 6** we sum up our result and discuss suitable future work on this research.

Chapter 2
Literature Review

Literature Review

A lot of work on the same problem was done by many researcher they all had the same objectives as ours. In this section we give an overview of the related work in the same field.

From 1990 to 2005

In the work of Sahiner et al [11] they prove through their different experiments that without using any CAD system performance of a doctor/physician in diagnosing/detection of lungs nodules are lower than the one who uses CAD scheme for lungs nodule detection. Detection of precise lungs nodules to allow the recognition of lungs cancer at starting stage that could direct to a larger number of endurance which provoked many researchers to find new methods of lungs nodule detection with the help of Computed Aided Detection (CAD) system [15-18].

In Jeong et al [19] and Reeves et al [20] further works on lungs nodule detection. They uses automatic lungs segmentation techniques to detect lungs nodule detection. Due to lots other body structures and many other interfering elements like noises in image, different features of images such as thickness of the slices, dimension of their pixels etc, nodule location and some other body structures which are directly connected to the nodules candidates also some of them have the same intensity, so detection of nodules with all these thing is a difficult job. So Jeong et al [19] and Reeves et al [20] focus on segmentation of lungs to detect lungs nodule detection. Cluster based automatic segmentation by using fuzzy c-mean is used by Antonelli et al [21] with the help of morphological analysis of resultant images.

Armato and Sensakovic [30] demonstrated the significance of sufficient division of lungs in PC helped identification and/or analyzing frameworks. His studies exhibited that up to 17% of lung handles/knobs can be lost in the midst of lung division if the count is not changed as per the task of handle area. A unimaginable test is the division of lungs affected by high thickness pathologies joined with their breaking points. Because of the absence of complexity among these pathologies and the tissues neighboring the lung, thickness based strategies come up short in this area. For this situation, it is fundamental some version method, at the same time, even along these lines, part of the lung is typically lost [31]. Because of the extensive measure of air in the lung, its inside has dim tonality in CT pictures, contrasting from the area around it. Along these lines, contrast in the middle of lung and neighbor tissues is the premise for large number of lung

division systems. Most routines depends on standards [32–34]. The lung area can be found by two ways [31]. The first is by method for district developing beginning at trachea. The second one, more regular, utilized thresholding and limitations as a part of size.

To discover nodules candidate, the fundamental methods utilized are different thresholding [35–38], numerical morphology [39–42], grouping [43–46], investigation of joined components in thresholded images[47,28], location of sphere in thresholded pictures [49] and utilization of accentuation channel with round structure elements[50–52].

Bae et al.[55] introduced a PC helped determination (CADx) for high-determination CT pictures (HRCT - high-determination processed tomography) utilizing two-dimensional and three-dimensional examination calculations. Bae et al [55] CAD system was tried in eight lung malignancy patients' data and acquired 95% of true positives and 0.91 FP/slice.

Hu et al.[60] developed a completely mechanized lung division strategy utilizing blends of morphological procedures to guarantee the incorporation of juxtaplueral knobs. The viability of the morphological procedures is reliant on the form and the span of the chose organizing component. As juxtaplueral knobs fluctuate fit as a fiddle, selecting an ideal size and shape that functions admirably in all scenarios is troublesome. For example, a littler measured organizing component will neglect to catch bigger estimated juxtaplueral knobs; on the other hand, a huge organizing component will bring about over-division and mutilation of the neighborhood district. Kim et al.[61] present a form walking strategy to stay away from fringe knob prohibition close to the lung limit. This technique tracks the projection limit to recognize suspicious zones with surface components like a genuine knob. A district developing system is connected to each distinguished zone to re-incorporate it as a component of the lung locale. Especially, composition includes alone can't identify all juxtapleural knob districts along a limit. Characterizing the quest window and edge for area developing strategy are likewise characteristic difficulties to this methodology. Ko et al. [62] utilize an ebb and flow based strategy to amend the starting lung veil. The ebb and flow for every point on the limit is computed to distinguish a quick change and a section is embedded to right such areas.

Suzuki et al. [63] developed a method based on machine learning, recognized as huge preparing counterfeit neural system, which improves the knob force and takes out different sorts of non-knobs. The PC tomography picture is utilized as a part of this examination. The diverse essential

picture handling procedures are utilized for expectation reason. In the first stage the noise ir removed from picture. In second stage lung locale is isolated from encompassing life structures. Near the beginning identification of pneumonic knobs for the analysis and treatment of lung disease. Bastawrous built up a CAD framework utilized for the identification of Ground Glass Opacity (GGO) knobs in mid-section CT pictures [68].

2006 and Afterward

In the literature different researchers shows that, by using the CAD systems help the physicians in the recognition [11-13] and analysis of lungs nodules [14]. The thinking at the back of these CAD frameworks is the proposition of an assistance to expert doctors, whether to highlight suspect radiologist ancient rarities or to offer a second feeling to the determination authority.

A.E.-B.G. Gimelfarb et al utilizes programmed division of low-dosage CT pictures. They utilizes data from probabilistic models made to control the development of a deformable model, in this model segmentation of lungs nodule was done with 0.96% mean error and with 1.1% stand deviation with respect to the specialist described format. Segmentation based on rules with template matching and Genetic algorithm was introduced by Ozekes et al.[23], and the result of this techniques are significant. Their framework accomplished 93.4% affectability and 0.594 false positives for each exam. Utilizing layout coordinating and including a hereditary cell neural system and edge in light of fluffy guidelines, Ozekes et al.[24] accomplished 100% affectability and a rate of 13.375 false positives for every case. Same work done by Li et al.[14] and he got 86%, 81%, and 75% affectability, with bogus positives of 6.6, 3.3, and 1.6 for every exam, individually, in a plan of fourfold cross-approval. Pu et al [25] tried their system on 52 pictures which comprise of 184 lungs knob applicants. They accomplished great result i.e. 95.1 % affectability with a mean of 1200 voxels per examine. They utilizes a marked separation field as a part of complete arrangement of CT pictures and recognized maximums establishes as potential knob hopefuls. Knob hopeful recognized by Pu et al [25] were positioned according to their separation to middle tomahawks, which is acquired by grouping procedure and application walking calculation. Fiebich et al [26] introduced a CAD scheme which consider low dose active contour images with a multi-thresholding algorithm. It is started from auto obtained value and from that point which was matched to a circle. The results of this CAD schemes are 58% sensitivity with 1.38 false positives per scan. Opfer et al [27] uses the technique which was

evaluated on LIDC (Lungs Image Database Consortium) database. In LIDC database ground truth is given by four radiologists. In their work they shows that their developed CAD technique was able to detect lung nodule candidates with 89% true positives and an average 2 false positives per scan. They detected nodule candidates having size of 4mm or larger. In the work of Sua'rez- Cuenca et al [28], they introduced a CAD scheme which is based on six classifiers: three support vector machines, linear discriminant analysis (LDA), quadratic discriminant analysis (QDA) and last one is ANN (Artificial Neural Network). They tested their technique/scheme on LIDC database and achieved 80% sensitivity with following false positives for each classifier: a) 23.7 for SVM-dot, b) 17.0 for SVM-poly, c) 23.35 for SVM-ANOVA d) 6.1 for LDA, e) 19.9 for QDA and f) 8.6 for ANN. Consolidated false positives were was 3.4 for the dominant part vote standard, 6.2 for the mean, 5.7 for the item, 9.7 for the neural system, and 28.1 for the probability proportion strategy.

The, work of Beigelman-Aubry et al.[29] showed appraisal of nodules areas and its response time when performed by physician with and without usage of an electronic structure. The work exhibited that the system upgrades the sensibility of the acknowledgment, what brought the trust between time up in 2%. Among the examinations with 109 patients, there was a handle which was not recognized by one of the radiologists, yet rather was distinguished by the system. Likewise, the usage of the system lessens broadly the time required by the experts to dismember the exams.

In Osman et al.[53], for every cut, areas of interest (ROI) were found by utilizing thickness estimations of the pixels and breaking down their eight bearings. The combination of all cuts shaped 3D ROIs, which contrasted with a knob model (format) permits distinguishing the knobs. Sensibility came to 100%, however the test information were confined to total six different scenarios. Retico et al.[54] proposed a framework in view of accentuation channels for circular articles and a neural order in light of voxels of chose locales to lessen false positives. The framework execution was assessed in an arrangement of information from 39 CT and has achieved almost 85% sensitivity with 10 to 13 false positives per exam. Dolejsi et al. [56] built up a PC supported determination framework taking into account morphological procedures and channels, trailed by the characterization of competitors by the AdaBoost classification module. The affectability accomplished was of 89.62% with 12.03 false positives for every picture.

Dolejší and Kybic [57] displayed a classifier intending to diminish the quantity of FP (False Positives) reactions of the essential indicator. The new classifier essentially lessened the quantity of false positives to 2.6 for every cut. de Oliveira Campo et al. [58] added to a technique in light of the bunching of comparative focuses in the picture, obeying comparability models. These models decide the way every locale of the picture will be grouped (as knob and non-knob applicants) and are characterized by a few descriptors. The principle descriptors incorporate change, extension and circular lopsidedness. Thus, the blend of these three descriptors prompted an affectability of 80.9%, along the 0.23 FP/slice.

Netto et al. [59] suggest a philosophy for programmed locations for lungs nodules. The developed strategy comprises of obtaining of registered tomography pictures of lungs, diminishment of the volume of enthusiasm through thorax extraction methods, separation of lungs portion, and recreation of the first state of the parenchyma. Then developing Growing Neural Gas is connected to compel much more the formations that are denser than the aspiratory parenchyma (knobs, veins, bronchi, and so on.). The accompanying stage is the partition of the structures taking after lung knobs from different structures, for example, vessels and bronchi. At last, the formations are delegated either knob or non-knob, through shape and composition estimations together with the bolster vector machine. The technique guarantees that knobs of sensible having larger size are detected with 86% affectability and 91% specificity. This outcome in a mean precision of 91% for ten preparing and testing explores different avenues regarding an example of 48 knobs happening in 29 exams. The rate of false positives per exam was of 0.138, for the 29 exams inspected.

Riccardi et al. [64] proposed a knob discovery system taking into account 3-D quick spiral sifting and scale space examination. As of late, mass-spring model-based division and applicant location routines have been proposed [65]. After knob applicants discovery, there are numerous false positives that require disposal. Over the previous few years, a few component extraction strategies and characterization systems have been proposed to lessen false positives. As a rule, the reported CAD frameworks fragment the recognized knob applicants, and afterward components are extricated from the divided knob competitors. These elements might be identified with the geometry (volume, sphericity, span of the proportional sphere,maximum smallness, greatest circularity, and most extreme unusualness), dim level (mean inside of the

sectioned item, standard deviation, and snippets of dark level), and by an iris channel and morphological components.

Pohle and Toennies [66] propose versatile district developing for division of therapeutic pictures. In this paper we propose a programmed procedure utilizing district developing and morphological operation, where the area developing calculation gains its homogeneity standard consequently from attributes of the locale to be divided and area properties are computed to distinguish the knob hopefuls.

Swati et.al proposed a lung tumor order framework [67] helps doctor to remove the tumor district and assess whether the tumor is favorable or threatening.

Dehmeshkiet al. [69] presented a CAD plan named as hereditary calculation format coordinating for programmed recognition of lung knobs. On the premise of geometric state of voxels and with the worldwide conveyance of knob power performs calculation of wellness capacity. Da Silva Sousa et al. [70] presented a CAD plan in which perform division at numerous stages. Every division stage is in charge of particular segments of the volume of CT image.Ye et al.[71]proposed a CAD sachem in which he utilized five elements containing force data, shape record and 3D spatial area. Opfer and Wiemker [72] demonstrates that consequences of CAD plan is straightforwardly identified with the extent of lung knob, demonstrating that 89% affectability can recognize knobs having size more noteworthy than 4mm and 60% affectability for having measurement under 4mm.Nie et al. [73] perform bunching makes utilization of mean-movement grouping and meeting list assets, building up a CAD framework that gives great results in the discovery f knobs process with the affectability of 89%. Messay et al. [74] connected various dim level limits to the volumetric lung areas to distinguish knob hopefuls. Likewise, various format coordinating based routines have been concentrated on. Xiaomin et al. [75] Introduces a technique and isolates it into three stages. In the first stage, a 2D multi-scale channel is utilized. In second stage, blob-molded knobs and on-knobs are separated. In the third and last stage, the shape elements of every area are extricated, and a classifier in view of mechanized standards to decrease false positives is connected. The strategy was connected to 30 exams and displayed an affectability of 100% and false positive rate of 8.4 for each exam. The CAD proposed by Tan et al. [76] depends on neural system and hereditary calculation furthermore incorporates developments, for example, the utilization of another classifier of

particular elements depicted as highlight deselective neuro-advancing enlarging of topologies. Two different classifiers are additionally utilized, to be specific settled topology manufactured neural systems and SVM. The procedure executed by the CAD comprises of four stages: preprocessing, recognition of knob applicants, highlight determination, and characterization. The model was accepted by the affectability calculation (87.5%). In Lee et al. [77], a course of action of classifiers called sporadic woods was used as a piece of two stages. The first was the period of area of lung handles, and the second one was the period of decline of false positives. The results got by this framework were of 100% for bona fide positives and 1.4 false positives for every picture. Camarlinghi et al. [78] propose the mix of various CAD frameworks expecting to give upgraded backing to lung knob ID. Their analysis was then contrasted with consequences of the individual frameworks by method for the ROC bend. The outcomes recommend that the higher the quantity of CAD frameworks utilized as a part of the identification, the higher the quantity of genuine positives, 65, and the lower the quantity of false positives, 139, over a LIDC base of 69 pictures containing 114 lung knobs. Chama et al. [79] present a system that uses mean-movement took after by methods in view of geometric properties, for example, district of interest (ROI), made from the symmetric centered guide of two typical topics. To accept the execution, 429 pictures (133 ordinary and 296 strange) from the LIDC-IDRI and Interstitial Lung Disease (ILD) databases were utilized. The proposed technique accomplished sensitivities and specificities of 97% and 99% (ordinary pictures) and 83% and 99% (unusual pictures), separately.

Wook Jin et al. [80] introduced a hereditary programming-based component change and grouping for the programmed identification of pneumonic knobs on processed tomography pictures. This CAD plan is partitioned into three fundamental steps. In initial step lung division is performed utilizing thresholding and 3D part marking. In second step ideal thresholding and manage based pruning for location of knob applicants are utilized. In third and last step he prepared a GP-based classifier to order knobs and non-knob competitor. Here every progression of this CAD plan is in a matter of seconds talked about. In the first part which is the division of lung, low thickness locales are isolated from high thickness districts utilizing thresholding procedures. After this 3D-joined segment naming is connected to independent the lung cover which is further cleaned by form revision process and after that it is utilized to concentrate lung volume. Exactness rate of knob identification is for the most part reliant on the lung division. In

the second part of this CAD plan, components of knob hopefuls are removed. In this progression, on the premise of sectioned picture volume ROIs are separated utilizing an ideal thresholding method. After this knob applicants were recognized and sectioned utilizing guideline based pruning. Guideline construct pruning was performed in light of the premise of various properties of knobs. In the third and last step a hereditary programming classifier (GPC) is prepared to uproot false positive decrease. GPC ideally chooses sufficient components from the info highlights and joins them with arbitrary constants and scientific administrators.

Chapter 3
Problem Statement

3.1 Problem Statement

In the work of Wook Jin et al. [80], certain shortcomings exist in the segmentation and classification procedures.

Wook Jin et al. [80] presented a hereditary programming-based element change and characterization for the programmed recognition of aspiratory knobs on registered tomography pictures. This CAD plan is isolated into three primary steps. In initial step lung division is performed utilizing thresholding and 3D part naming. In second step ideal thresholding and govern based pruning for discovery of knob hopefuls are utilized. In third and last step he prepared a GP-based classifier to group knobs and non-knob hopeful. Here every progression of this CAD plan is in a matter of seconds talked about. In the first part which is the division of lung, low thickness areas are isolated from high thickness locales utilizing thresholding procedures. After this 3D-associated part naming is connected to discrete the lung cover which is further sanitized by shape redress process and after that it is utilized to concentrate lung volume. Precision rate of knob discovery is for the most part subject to the lung division. In the second part of this CAD plan, elements of knob competitors are extricated. In this progression, on the premise of fragmented picture volume ROIs are extricated utilizing an ideal thresholding method. After this knob competitors were distinguished and fragmented utilizing standard based pruning. Guideline construct pruning was performed in light of the premise of various properties of knobs. In the third and last step a hereditary programming classifier (GPC) is prepared to uproot false positive lessening. GPC ideally chooses sufficient components from the information highlights and consolidates them with arbitrary constants and numerical administrators.

Although this CAD scheme is one of the good scheme but there are some shortcomings in this technique which need to be improved. The major problem of this technique is it cannot detect larger juxtavescular nodules because of their complex structure. In this CAD scheme larger juxtavescular nodules are considered as non-nodule candidates. Another problem is that the separation of nodule candidate from non-nodules are performed using rule based pruning and in rule based pruning larger objects are categorized as non-nodules (vessels, bronchi or other structures) so this technique is not able to detect larger juxtavescular nodules.

For example:

LIDC-IDRI-0001

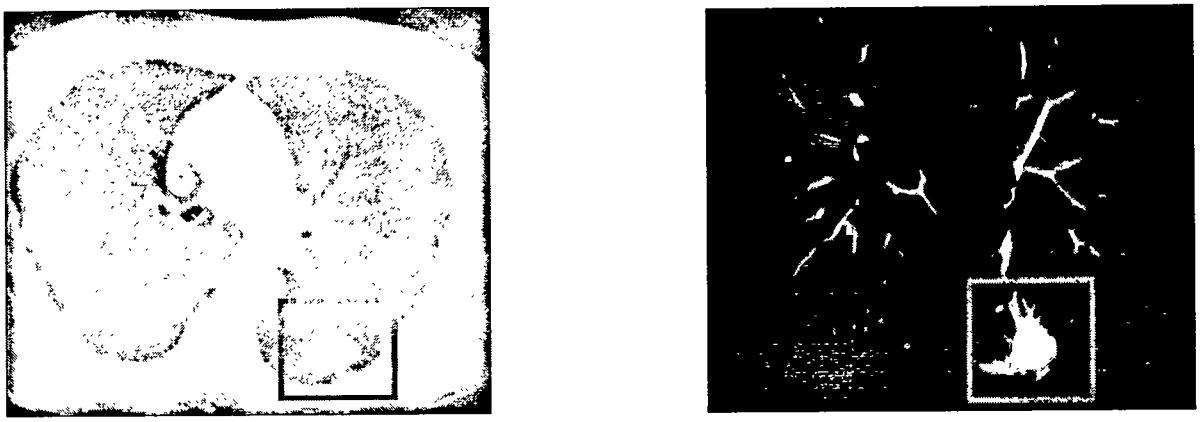

(a)Segmented lung Image (b) ROI

Fig. 1

In Fig.1 (a) and Fig.1 (b) juxtavescular nodule can be seen close to pleural wall which is very visible, large in size and spherical in shape. After implementation of Wook Jin et al. [80] CAD scheme, the study finds that some of the Juxtapleural nodules are not detected by the Wook Jin et al. [3] CAD scheme. Fig 1 shows one of the example of such type of nodules which cannot be detected by Wook Jin et al. [80] technique.

Another drawback of this technique is it can detect solid nodules but unsuccessful to detect non-solid nodules which have low visibility.

For example:

LIDC-IDRI-0002:

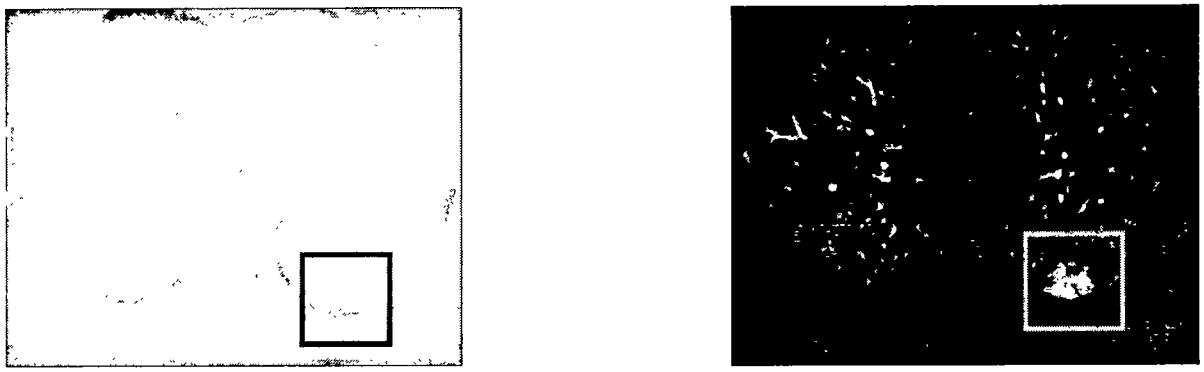

(a) Segmented lung Image (b) ROI

Fig. 2 a) Segmented lung image. b) Image after Region of Interest

In fig. 2a (image after segmentation process) and fig. 2b (image after ROI extraction) a large sized non-solid juxtapleural nodule which have low visibility can be seen easily but not detected by Wook Jin et al [80] technique.

Chapter 4
Proposed Methodology

Proposed Methodology

In the fourth chapter we described the planned technique of our CAD scheme for the detection of nodules from CT images. The major contribution of this methodology is: it not only focus on a single type of nodules, this hybrid approach for nodule detection can detect all types of lung nodules which includes isolated nodules, juxtapleural nodules and juxtavescular nodules. Another major commitment of this strategy is it can likewise identify large size of juxtavescular nodules which are not detected earlier in any technique because of their complex structure. Juxtavescular nodules are on the grounds that connected to alternate structures, for example, vessels and bronchi tree so in literature there is no any technique which mainly focuses on the larger size of juxtavescular nodules.

There are four major steps in our proposed methodology these are as follows: First one is Lung Segmentation in which we used linear interpolation and lung parenchymal identification techniques, Second one is detection Region of Interest in which we performed three processes that is Multiple threshold for ROI, Contour correction and seed point choice, Third one is the process of Nodule Detection in which we used two different models for detection of different types of nodules we used Deformable model for detection of Juxtapleural nodules and isolated nodules and second model is Distance Transform for juxtavescular nodules detection and Fourth step which is actually the last step in False positive reduction using rule based pruning. Graphical representation of our proposed methodology is given below:

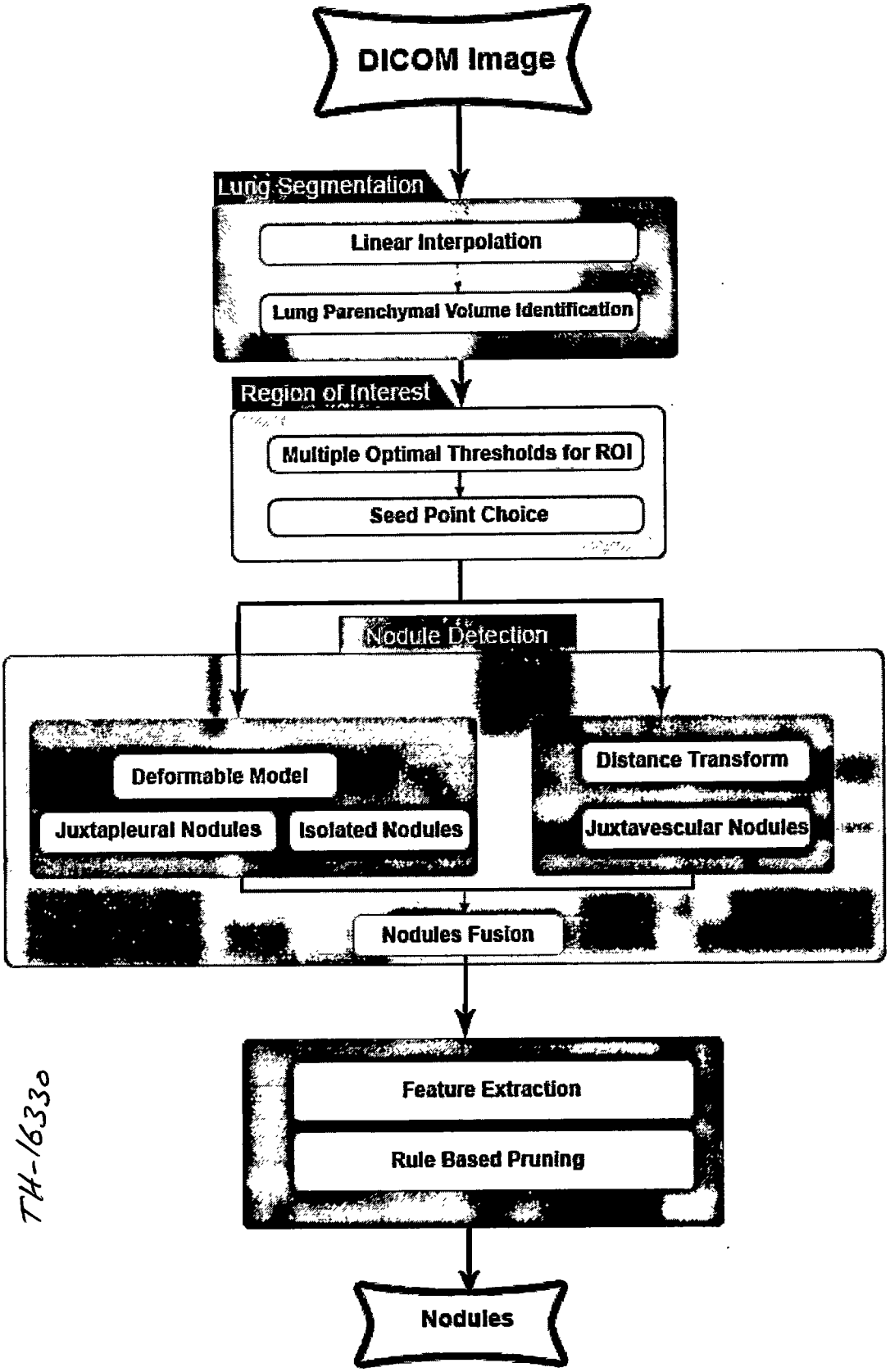
DICOM Image
Lung Segmentation
Linear Interpolation
Lung Parenchymal Volume Identification
Region of Interest
Multiple Optimal Thresholds for ROI
Seed Point Choice
Nodule Detection
Deformable Model
Juxtapleural Nodules
Isolated Nodules
Distance Transform
Juxtavescular Nodules
Nodules Fusion
Feature Extraction
Rule Based Pruning
Nodules

4.1 Linear Interpolation:

In the advancement of a CAD framework for the most part identification plans are depends on the examination based on volume of Computer Tomography pictures in this way as a matter of first importance we change over all voxels into 3D coordinate system network with uniform 3D spatial determination to evacuate the conceivable events of blunder because of anisotropic representations of lattices. There is a few addition methods were presented in the writing yet here in our work we utilized straight introduction in view of its computational effortlessness furthermore this strategy is broadly utilized for information recreation. By thought the spatial determination along the hub heading in CT examination is typically not quite the same as the spatial determination inside of every cut that is the reason we perform a straight addition along the hub bearing. Introduced cut is figured between all matched neighboring cuts. Subsequent to applying of direct addition size of each voxel is cubic.

4.2 Lung Parenchymal Volume Identification:

In any CAD scheme lung segmentation is very necessary because to detect nodule from input image as a whole is a difficult task. That's why we have to segment input image into different slice to minimize to calculation period and FPs. In this section we have to find initial volume of interest (VOI). Major objective of separation of lungs portion of the input image is to better identification of juxtavescular nodules, isolated nodules and juxtapleural nodule. After segmentation of the input image it is a little bit easy to find all different types of nodules from the image. There are lots of techniques were described in the literature for lung segmentation. The most commonly used technique is threshold based region filling. Although this technique is efficiently segment the lung parenchyma but it also erroneously remove important regions. Most commonly it excludes juxtapleural nodules for the reason that juxtapleural nodules are attached with the pleura. Simple thresholding and filling technique or algorithm is not able to detect juxtapleural nodules separately. That's why to overcome this problem we used an algorithm based on following two steps:

- Inclusion Process

  A 3D Region Growing algorithm is used for lung parenchyma identification.
- Connectivity Analysis

To incorporate interior structures with high power esteem (knobs and vessels) and pleura layer neighboring inward lung volume a widening procedure is connected which is called Connectivity analysis.

Now brief descriptions of both above processes are given below:

4.2.1 Inclusion Process:

Bronchial tree and air lies in the interior lung volume and in CT Images they are spoken to as low power voxel encompassed with the high force voxel which are relate to the pleura surface. By examining this we perform division of the interior lung volume by the method for a 3D RG (Region Growing) calculation. RG can make locales with comparable characters. By guideline that is: begins from a seed point and district is incremental appending so as to develop to every start those adjacent focuses which have comparable properties to the seed. This iterative procedure is proceeding until there are no more focuses fulfilling the predefined criteria. Presently the most critical thing which straightforwardly impacts on the execution of RG (Region Growing) calculation is to pick better incorporation process with proper seed point. For our situation we utilize Simple Bottom Threshold (SBT) as consideration principle. In the event that the power I of a nonexclusive voxel is lower than the edge esteem than this voxel is added to the area developing. For this reason estimation of limit is consequently chosen by the system proposed by Ridler et al [16] after an iterative process This procedure depends on the CT voxel dim quality circulation which comprises of two one of a kind parts: one have air, lung parenchyma, trachea and bronchial tree and the second one comprises of vascular tree, bones, muscles and fat. The ideal edge is set between these two locales. Presently go to the determination of seed focuses for the calculation. RG calculation utilizes two seed focuses, determination criteria of seed point is quickly depicted by D. Cascio [17] which have taking after steps:

- **set the begin point on the focal voxel (P0) of focal cut of the output;**
- **shift to one side of a voxel;**
- **if the consideration guideline for such voxel is fulfilled, then begin the RG, else go to the stride 2;**
- **if, toward the end of the recursive procedure of RG, the volume (in voxel) chose by the RG process has the same request of size with the normal lung volume, the trial stage closes else go to the stride 2.**

A data on the lung volume's request of greatness is gotten from the histogram of the CTs dark tones, by evaluating the territory under the second top from the left (red district in Fig. 3). This part of the dispersion, actually, alludes accurately to the voxels having a place with the lung parenchymal and bronchi

To select the required volume of pulmonary, all the above steps are repeated. Below Fig. 2 displays example of inclusion process.

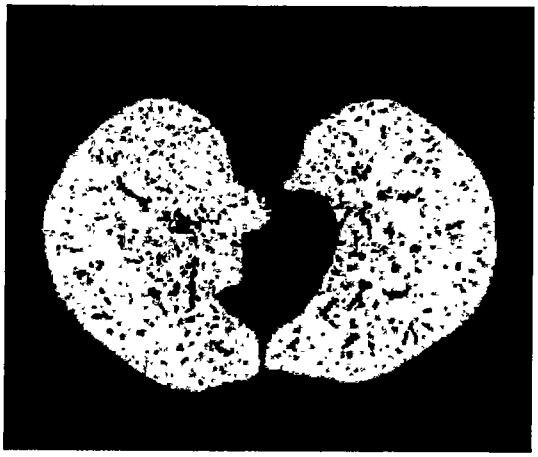

Fig. 2. Image after inclusion process

4.2.2 Connectivity Analysis:

After the inclusion process we get the segmented image but in this image internal nodule, vessels and air walls are not included. So to include these nodules a dilation process called connectivity analysis is applied to on lung image. To make volume of interest more accurate this connectivity analysis is applied. After applying connectivity analysis juxtapleural nodules are also included into the segmented image. Fig. 3 represents the example of volume reconstruction.

4.3 Multiple Optimal threshold for ROI extraction:

There are different intensities of nodules and varying level of vessels attachments therefore to extract Region of Interest (ROI) in such situation we use multiple threshold. In the literature a fixed value for multiple thresholds is used, but in our work we use optimal threshold to detect ROI. Steps to find optimal threshold algorithm is as follows:

As we know that thoracic CT consists of two main group of pixels. First one is high intensity pixel located in the body (body pixels) and second is low intensity pixels which are in lungs and

surrounded air which are called non-body pixels. Larger intensity difference between these two group of pixels therefore thresholding is a best mechanism to separate these groups. In literature Wook Jin et al [80] uses five static threshold values which is not optimal threshold. In our technique we use the method of optimal thresholding defined by Hu et al [60]. This technique iteratively figures the estimation of a limit so that the two gatherings of pixels are all around isolated.

Let T^w be the edge esteem at step w and μ_a , μ_b be the normal power estimation of body pixels(i.e. with force higher than T^w), separately non-body pixels (power lower than T^w). The limit for step $w+1$ is:

$$T^{w+1} = \frac{\mu_a + \mu_b}{2}$$

This technique is rehashed until union i.e. until step e where $T^e = T^{e-1}$. The introductory limit T^0 is set to 128 which is middle dim level. At the point when joining is finished, the picture is thresholded at quality T^e. Body pixels are set to 0 and non-body pixels are set to be 1.

Pseudo Code of optimal threshold algorithm is:

```
function opt_threshold = comp_optThreshold(T0)
  global J;
  global rows cols;
  Tp=-10;
  Tc = T0;
  flag=0;
  while(Tp~=Tc)
    Mo=0;  oc=0;  bc=0;  Mb=0;
    %threshold using Tp
    for i=1:rows
      for j=1:cols
        if (J(i,j)<=Tc)
          J(i,j) = 255;
          Mo = Mo + J(i,j);
```

```
            oc = oc + 1;
          else
            J(i,j) = 0;
            Mb = Mb + J(i,j);
            bc = bc + 1;
          end
        end
%         Mo = Mo/oc;
%         Mb = Mb/bc;
        Tp = Tc;
        Tc = (Mo+Mb)/2;
      end
    end
    opt_threshold = Tc;
end
```

4.4 Seed points choice:

In this area we select some seed focuses which will be utilized as a part of the following segment "Deformable Model" as information. As we probably am aware knobs have more prominent force as for the pneumonic parenchyma and they can be effortlessly found by searching for neighborhood maxima in the volume of interest which we got after the network investigation process. So a voxel level operation is performed on the accompanying grids:

$$O(a,b,c)= (M(a,b,c)- N(a,b,c)) . I(a,b,c) \quad (1)$$

Where M(a.b,c) is the matrix after connectivity analysis process, N(a,b,c) is the matrix we get after RG process, I(a,b,c) is the input image, and O(a,b,c) is the resultant matrix. Fig.3 represents the result of equation (1). After getting matrix O(a,b,c) we apply a hit the highest point detector algorithm on it to discover confined maxima and select seed points which will be used in the next step.

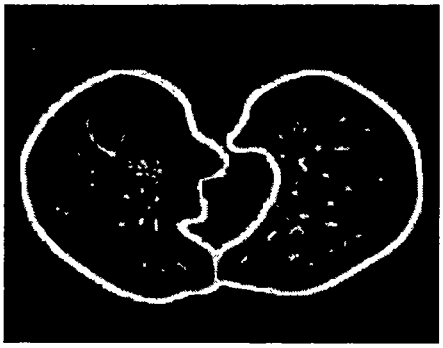

Fig 3:

4.5 Nodule Detection:

In this process we detect nodule candidates from other structures. As we mentioned earlier that methodology which we used in our CAD system can detect all the possible types of nodules like: isolated, juxtapleural and juxtavescular nodules. To detect these nodules we uses two techniques, first one is deformable model to detect isolated nodules and juxtapleural nodules and second one is distance transform to detect juxtavescular nodules. Detail description of these methodologies is described below:

4.5.1 Deformable Model:

By using this model our main focus is to detect isolated and juxtapleural nodules from the lung parenchyma this model is also called Mass Spring Model. The basic aim of deformable model is to identify the shape of object; here we use it to identify the nodule's shape among other structures. Deformable model is also known as snakes, which uses a-priori knowledge by definition and parameterization of an energy term as well as by the placement of the initial model in the images. Deformable model discover the balance between the inner strengths (portraying the model shape) and outer powers (depicting the picture data). In the material science based displaying worldview, the shape relates to connected (outside) powers on the deformable model and so that model is converges into the shape of object, while inside powers keep the model smooth amid disfigurement. Deformable model is adjusted considering the vitality term until the vitality is insignificant.

4.5.1.1 Design of Deformable Model:

As said before in this work we need to add to a legitimate arrangement of strengths or at the end of the day we need to locate a suitable vitality capacity from which we get answer for knob form. This model was introduced by D Casico et al [81] .They speaks to form by an arrangement of N mass focuses model vertices. As beginning 3D deformable model, we took a circle cross section of mass focuses. The fundamental objective of the model is, beginning from an augmented position the mass cross section holds to the potential knobs. Seed focuses which were picked in the past segment are taken as the focal point of every circle network. We marked the circle with N quantities of mass focuses that makes the dynamic model and with t number of mass purposes of the on a solitary cut that makes a connection $L=t.u$ where u is the total number of slices. Each mass in the sphere N(j) (j=1...t) is connected with two other masses N(j-1), N(j+1) which belongs to the same slice and with two slices N(j-n) and N(j+n) which belongs to the previous slice. We can write it in more generalized way as follows:

$$E_{functional}^{tot} = \sum_{i=1}^{N}[E_{internal}(i) + E_{external}(i)] \quad (2)$$

As shown in above Eq(2) every single element in the proposed models play an important role with both internal and external energies to the energy functional. Now we will describe internal and external forces in details.

4.5.1.2 Internal energy:

The internal energy $E_{internal}(i)$ of the deformable model and this model is executed by the calculation and addition of all following energies:

4.5.1.2.1 Elastic energy:

Elastic energy is the first step to get the form of the lung which is to be separated. The general peak i is associated to its four first siblings two in the xy-plane and two in z-plane. Those four points are contributes in the elastic energy.

$$E_{elas}(i) = \alpha[E_{spr,i-1}(i) + E_{spr,i+1}(i) + E_{spr,i-n}(i) + E_{spr,i+n}(i)] \quad (3)$$

Where $E_{spr\,j}(i)$ represents the elastic energy of the model which is attached with the two masses i and j.

$$E_{spr\,j}(i) = \frac{1}{2}k\Delta x^2 \quad (4)$$

Where Δx the distance between two mass points and k is is the spring constant, is a parameter.

4.5.1.2.2 Bending Energy:

Second step is to apply bending energy on the object. The model must adjust to the diverse bends that the item might show. In this way we apply bending energy. Here the bending energy is linked with general vertex *i* which is defined as follows:

$$E_{bend} = \beta\|P_{i-1} - 2P_i + P_{i+}\|^2 \quad (5)$$

where P_i indicates the position of *ith* vertex.

4.5.1.2.3 Attraction Energy:

Vertices belongs to same slice, the geometric center of those positions are taken as a linking point for the calculation to separate the vertices normal ($\bar{d}$) and standard deviation(σ_d). If the *ith* vertex have the distance d_i from the center then it can be represent as:

$$d_i > \bar{d} + \sigma_d \quad (6)$$

Then the attraction energy is linked with the *ith* vertex is given as

$$E_{attr}(i) = \gamma\frac{d_i}{\bar{d}} \quad (7)$$

With respect to average distance as far as vertex is from the center which caused the larger amount of energy contribution. This contribution makes the points on the model surface is almost spherical which are most likely nodules.

4.5.1.3 External Energy:

Internal energy evaluated the contour points regulates the contraction and bending but internal forces does not provides any pulling force from which we can separate our desired object from the rest of image. Therefore we apply external forces for this task. External energy $E_{external}$ is the combination of gradient and potential energies. Now we can describe the contribution of each energy in our work one by one respectively.

4.5.1.3.1 Gradient Energy:

Gradient energy makes the point of model with high gradient evolve towards the location. A very small amount of energy will be associated with the *ith* vertex if it is located on the edge point, which is represented by the following equation:

$$E_{grad}(i) = -\delta \|\nabla I(P_i)\| \quad (8)$$

where $I(P_i)$ is intensity of *ith* vertex at the P_i position.

4.5.1.3.2 Potential Energy:

Every point of models is linked with the potential energy and if the point is with high intensity than it means more energy is linked with it. So if a pixel moves from low intensity value to the large intensity value like the pleura surface then it must pay additional energy function such as:

$$E_{pot}(i) = I(P_i) \quad (9)$$

4.5.1.4 Energy Functional:

After calculation internal and external forces now we have to sum up all the energies to get the total energy function which can be represents as follows:

$$E_{fuctional} = \alpha E_{elas}(i) + \beta E_{bend}(i) + \gamma E_{attr}(i) + \delta E_{grad}(i) + \epsilon E_{pot}(i) \quad (10)$$

where α, β, γ, δ and ε are dimensional parameters empirically reduced. To identify the values of these parameters we introduced various sized artificial objects in the image like spheres which represents the isolated nodules and hemisphere which represents juxtapleural nodules. As the start of the methodology we mentioned that our aim is to detect isolated and juxtapleural nodules, so both these types of nodules were detected successfully.

Now for the detection of juxtavescular nodules we use the distance transform technique. Detail description of this technique is given in next section.

4.5.2 Distance Transform:

After applying deformable model we get the isolated, juxtapleural and some small juxtavescular nodules. Deformable model excludes larger juxtavescular nodules due to their complex structure,

In our proposed rule based pruning there are four rules R_1,R_2, R_3 and R_4 which are defined on the features of nodule candidates such as Diameter(l) , Area(l), Volume(l), Elongation(l) and Circularity(l). To separate nodules candidates from non-nodule candidates each feature must be compared with a minimum and maximum value of threshold. Here we represents $T_a^{(min)}$,$T_d^{(min)}$ and $T_v^{(min)}$ as minimum thresholds for area, diameter and volume respectively. Similarly $T_a^{(max)}$, $T_d^{(max)}$ and $T_v^{(max)}$ represents the maximum threshold values of area, diameter and volume of nodule candidates respectively. If an object has less value of its diameter, volume or area from the threshold value than it is not a nodule candidate and if its diameter, volume or area value is maximum than the threshold value, than it is considered as non-nodule candidate.

Pruning Rules:

Rule R_1:

Diameter (l) < $T_d^{(min)}$

Rule R_2:

Volume (l) > $T_v^{(max)}$ or Overlapped (l, VS) > T_0 or (*Elongation* (l)>T_e *and Volume* (l)> $T_v^{(min)}$)

Rule R_3:

Diameter (l) >$T_d^{(max)}$

Rule R_4:

Circularity (l) >T_c and Area(l) > $T_a^{(min)}$ and Area(l) < $T_a^{(max)}$.

On the basis of all above four rules we will separate nodule candidates from the non-nodule candidates. Here is the algorithm of our rule based pruning.

Algorithm for Rule based pruning for separation of nodule candidates from non-nodules

1. **function** Pruning (*NFs*) →Remove vessels and noise (**Nodule Fusion(NF)**)
2. **for** each *NF* ε *NFs* **do**
3. $NC \longleftarrow \Phi$ → Nodule Candidates
4. $VS \longleftarrow \Phi$ → Vessels
5. **if** Diameter(l) < $T_d^{(min)}$ then
6. **continue** → Noise
7. **end if**
8. **if** Volume (l) > $T_v^{(max)}$ or Overlapped (l, VS) > T_0 or (*Elongation* (l) > T_e *and Volume* (l) > $T_v^{(min)}$) **then**
9. $VS \longleftarrow VS \cup \{l\}$ → Vessels
10. **continue**
11. **end if**
12. **if** Diameter (l) > $T_d^{(max)}$ **then**
13. **continue** → Noise
14. **end if**
15. **if** Circularity (l) > T_c and Area(l) > $T_a^{(min)}$ and Area(l) < $T_a^{(max)}$ **then**
16. $NC \longleftarrow NC \cup \{l\}$ → Nodule Candidates
17. **end if**
18. **end for**
19. **return NC**
20. **end function**

Chapter 5
Results and Discussion

Results and Discussion

In this area, we introduce the usage points of interest and various trial results at each substage of the proposed CAD framework. To start with, we display how to assemble the lung CT database and to decide its ground truth and hit criteria. Next, we examine the usage subtle elements and execution of the lung volume division strategy and the identification of nodule candidates.

5.1 Data Collection and Detection Criteria:

The execution of the proposed CAD framework is assessed utilizing the LIDC database [2, 15], a freely accessible database from the National Biomedical Imaging Archive (NBIA), and its nodules have been completely clarified by various radiologists. In this database, four master mid-section radiologists drew plots for nodules having viable sizes of 3 mm or more noteworthy. The ground truth was then settled by a visually impaired perusing and a resulting un-blinded perusing. The LIDC database comprises of 84 CT examines, however just 58 CT checks contain nodules. In the nodules containing CT filters, we arbitrarily gathered 32 CT examines with a specific end goal to assess the proposed framework. All commented nodules divisions were utilized as a part of the assessment of the proposed strategy. The covered manual nodules divisions from four distinct radiologists were converged to a solitary nodule division. Therefore, this dataset comprised of 76 nodules and 5453 slices, and the nodule sizes across went from 3 mm to 30 mm.

The nodule candidates were delegated nodules or non-nodules in view of annotation gave by the mid-section radiologists. Amid the assessment, each recognized knob hopeful was resolved to be a knob if its separation to any knob in the database was littler than 1.5 times the span of that knob, or if its range was more noteworthy than 0.8 times or littler than 1.5 times the sweep of the objective knob. We indicate this arrangement as a hit. We additionally took into consideration a 'close hit' by utilizing these 0.8 and 1.5 components, which were acquired by trials. On the off chance that a hit on a recognized knob hopeful was delivered, it was considered a TP; else, it was viewed as a FP.

5.2 Lungs Segmentation:

First of all we segmented lung volume based on linear interpolation. First of all we convert all voxels into 3D Cartesian coordinate grid with uniform 3D spatial resolution to remove the possible occurrences of error due to anisotropic representations of grids. According to our consideration the spatial resolution along the axial direction in CT examination is normally different from the spatial resolution within each slice that's why we perform a linear interpolation along the axial direction. Interpolated slice is computed between all paired neighboring slices. After applying of linear interpolation size of each voxel is cubic. After this we have to find lungs parenchymal volume for this purpose we used a two steps algorithm; 1) Inclusion process and 2) Connectivity analysis. In inclusion process we used 3G region growing algorithm and find Volume of interest (VOI) after it we perform a connectivity analysis process to include image internal nodule, vessels and air walls. For this purpose a dilation process called connectivity analysis is applied to on lung image. To make volume of interest more accurate this connectivity analysis is applied. Details of Inclusion process and Connectivity analysis is described in **Proposed Methodology Section**. Figure 4 represents different images of each stage.

Input Image | Inclusion Process | Segmented Image

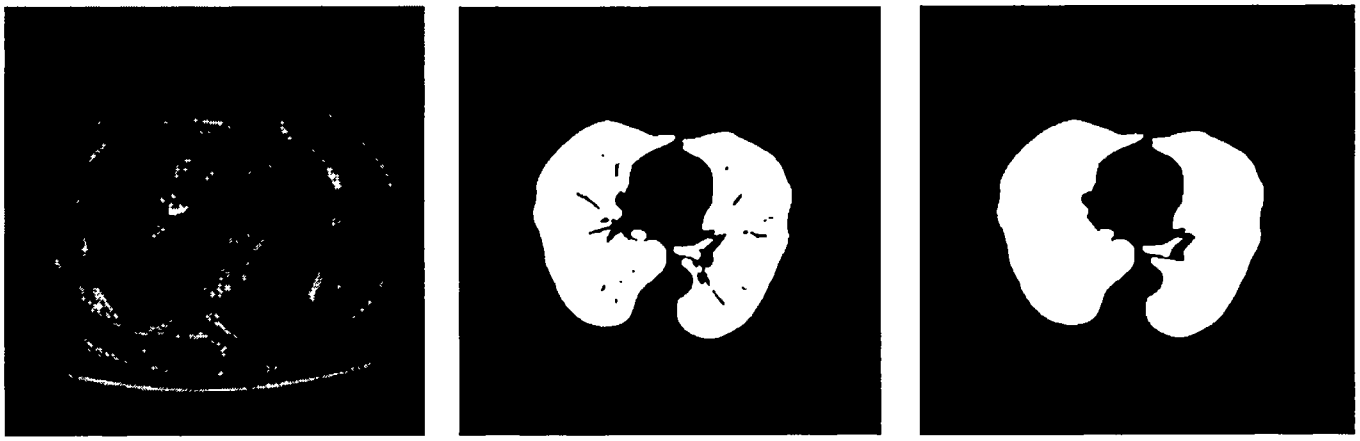

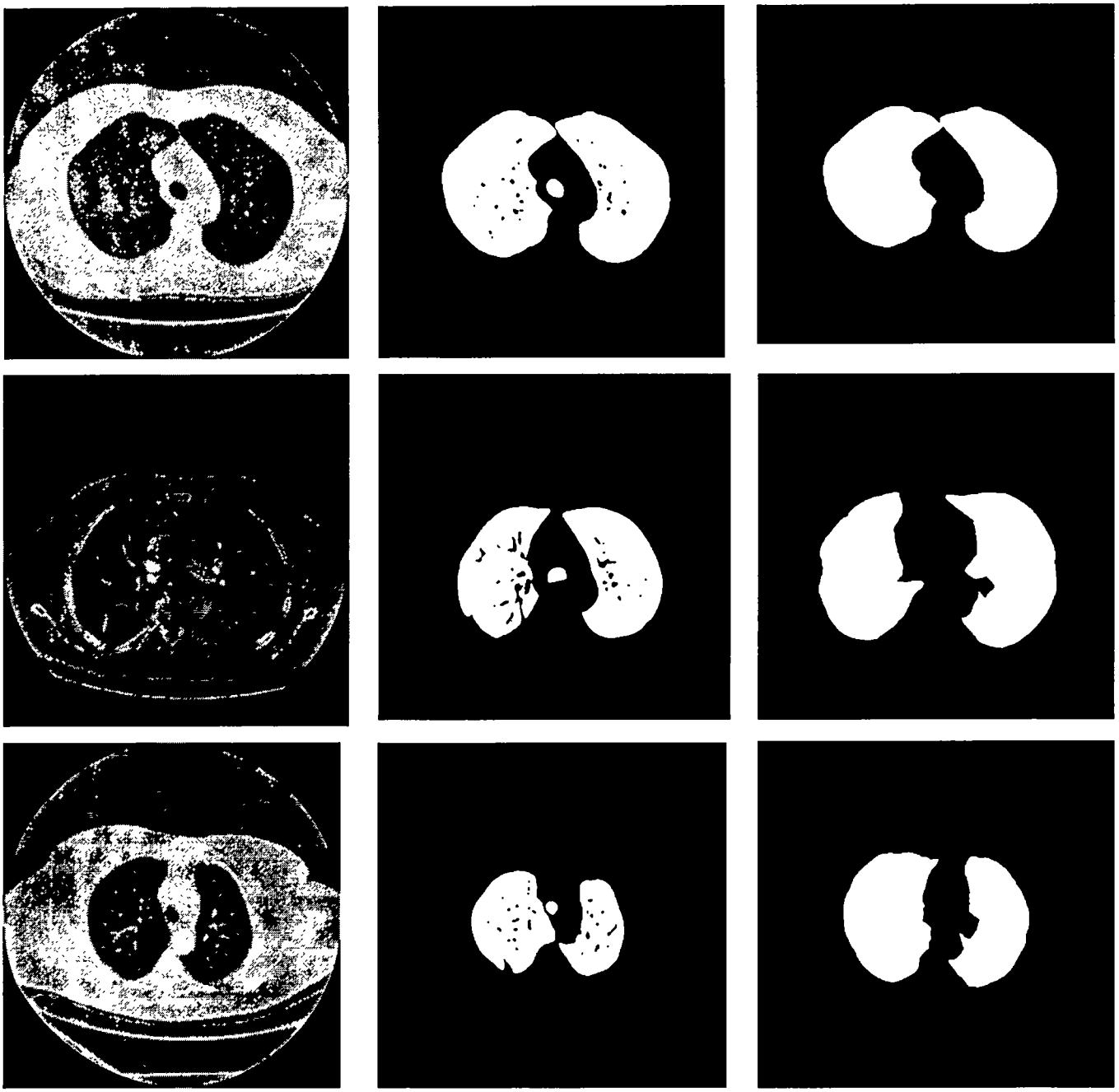

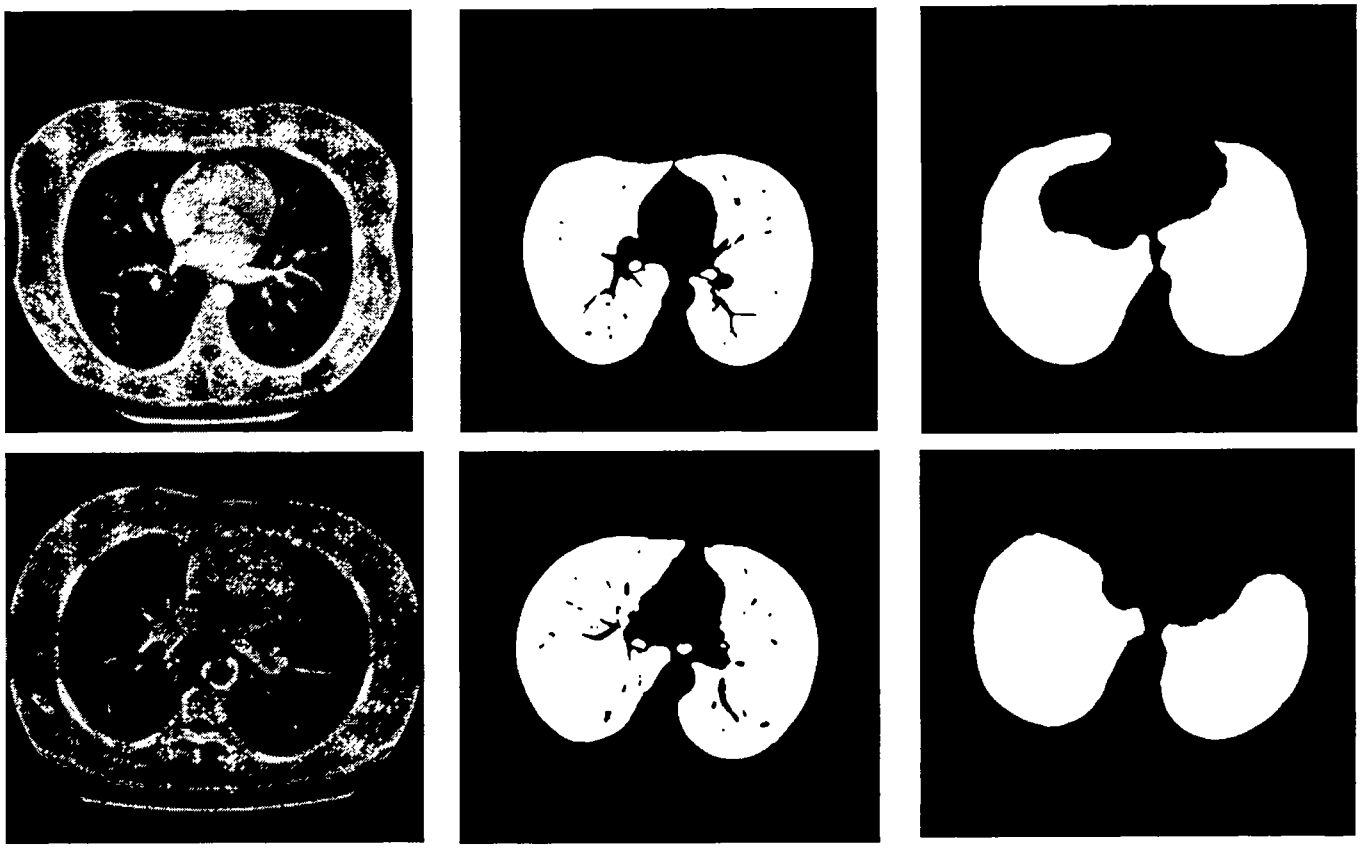

5.3 Region of interest Extraction:

After segmentation multiple optimal thresholding applied to extract region of interest(ROI). In earlier technique Wook jin et al [80] extracted ROI by giving five static threshold values which are not optimized. In our work we applied ROI algorithm to extract region of interest. Detailed algorithm is described Proposed Methodology Section. Resulted images of ROI are given below:

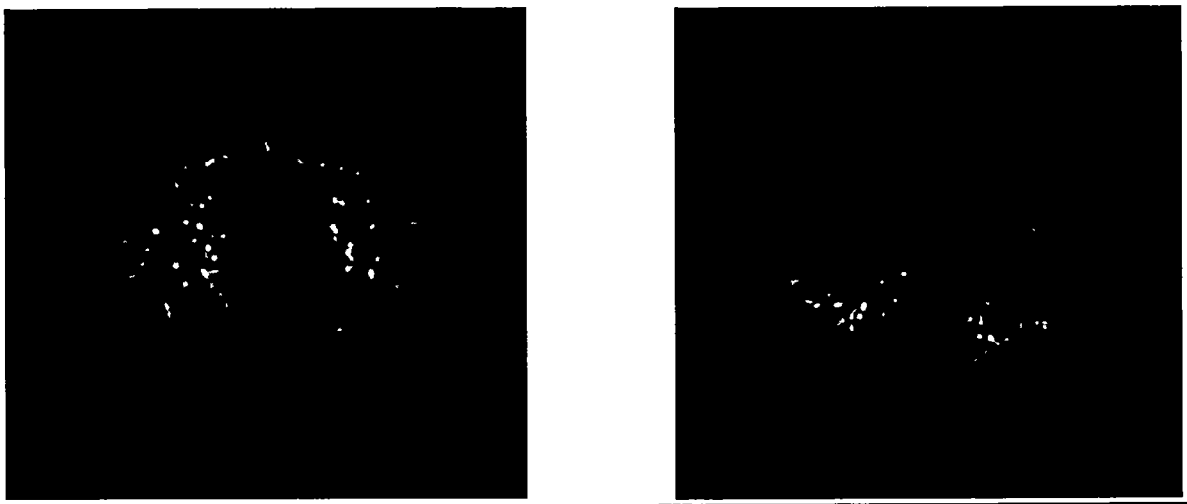

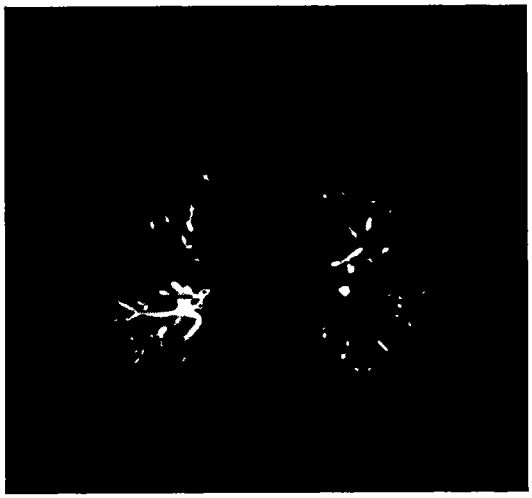

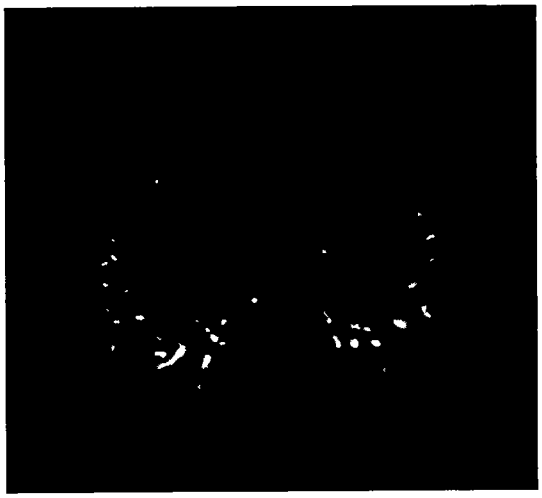

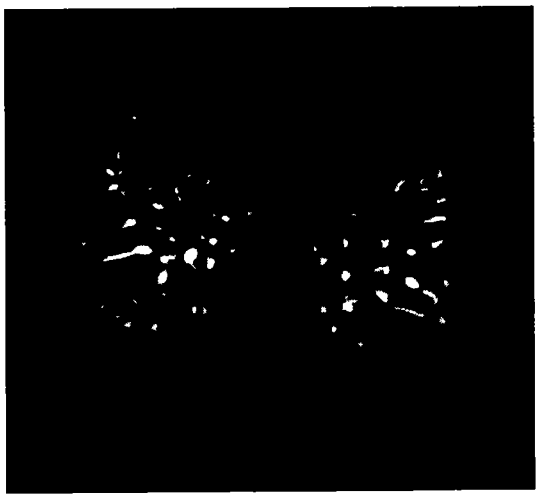

5.4 Nodule Detection

Deformable Model:

We planned a focalized strategy for the development of the deformable model from a starting state in which the vertices are laid out on a vast measured box (this crate can contain ROI sizes up to 50 mm). From this sort of starting condition the model is will completely expected to

merge towards the nonexclusive ROI shapes by a constriction. The technique we created has the accompanying properties:

- Low computational multifaceted nature;
- Easiness of execution;
- Excellent execution if the introduction of the model is most certainly;

The steps of the algorithm are the following:

- the value of the energy functional $E_{fuctional}$ (i) is initialized with the energy value calculated at the ith vertex (i=1, . . . ,N) of the initial sphere mesh;
- for each vertex, the algorithm evaluates the energy functional for the vertex itself and for its eight (first-order) neighbors belonging to the same slice (the generic vertex is allowed to move only within its own slice). The new vertex location is subsequently chosen as the lesser energy vertex among these nine possibilities. The iteration process finishes when a full cycle energy analysis of all the N vertices is completed;
- if a vertex remains stationary for two successive iteration steps, it will be artificially shifted by an applied "jolt"; the procedure corresponds to the broadening of the neighborhood where the energy functional gets estimated to successive orders of neighbors. For the energy analysis, these new locations are chosen along the direction towards the geometric center of the model;
- if the energy functional of N points resulting from Eq. (2) is less than the energy functional estimated at the previous iteration step, then the procedure returns to the step item (2), otherwise the minimization process ends.

Distance Transform:

The 3D distance transform also known as separation change [22] is computed in each of the structures portioned in the past stage, beginning with worth one, in all voxels of the edge, and is augmented as we move towards the inward voxels, until there is maybe a couple voxels left at the same separation from the edge. At the end of the day, voxels of a same layer have the same quality for the separation change. The computation closes when we achieve the most internal

layer. Tubular and prolonged structures have consistent estimations of the separation change with little interims along their more prominent length.

Following the distance transform is computed as for the edge of the structure, the estimations of most extreme grouping of voxels are in the focal point of the few structures found in the bronchial and vascular trees. These focuses are conceivable lung knobs. Thus, the nearby maximums are found along all structures of the bronchial and vascular trees and utilized as seeds as a part of the procedure of knob identification through 3D district developing. In any case, contingent upon the geometry of the fragmented structures, neighborhood maximums can show up in conglom-erates and, for this situation, they are dealt with as a solitary nearby greatest, however every one of them are seeds of the district developing calculation. The division of lung knobs from vessels, bronchi, and so forth., is finished by investigating the element of tube shaped state of vessels and bronchi. They have a steady esteem along their length, and a basic 3D district developing is equipped for confining a knob from structures joining with it.

Nodule Fusion:

At last nodule detected by deformable model and nodules detected by distance transform method are combined together.

5.5 False positive reduction using rule based pruning:

Nodule candidate detected at the pervious stage may include some non-nodule candidates, so to remove those candidates and to ensure accuracy of our detected rules here we perform rule based pruning. In other words to reduce false positives we perform rule based pruning.

In our proposed we used Wook Jin et al [80] rule based pruning there are four rulesR_1,R_2, R_3 and R_4 which are defined on the features of nodule candidates such as Diameter(l) , Area(l), Volume(l), Elongation(l) and Circularity(l). To separate nodules candidates from non-nodule candidates each feature must be compared with a minimum and maximum value of threshold. Here representations are as follows: $T_a^{(min)}$,$T_d^{(min)}$ and $T_v^{(min)}$ as minimum thresholds for area, diameter and volume respectively. Similarly $T_a^{(max)}$, $T_d^{(max)}$ and $T_v^{(max)}$ represents the maximum threshold values of area, diameter and volume of nodule candidates respectively. If an object has less value of its diameter, volume or area from the threshold value than it is not a

nodule candidate and if its diameter, volume or area value is maximum than the threshold value, than it is considered as non-nodule candidate.

Pruning Rules:

Rule R_1:

Diameter $(l) < T_d^{(min)}$

Rule R_2:

Volume $(l) > T_v^{(max)}$ or Overlapped $(l, VS) > T_0$ or $(Elongation\ (l) > T_e\ and\ Volume\ (l) > T_v^{(min)})$

Rule R_3:

Diameter $(l) > T_d^{(max)}$

Rule R_4:

Circularity $(l) > T_c$ and Area$(l) > T_a^{(min)}$ and Area$(l) < T_a^{(max)}$.

On the basis of all above four rules we will separate nodule candidates from the non-nodule candidates. Here is the algorithm of our rule based pruning.

Algorithm for Rule based pruning for separation of nodule candidates from non-nodules [80]

1. **function** Pruning (*NFs*) →Remove vessels and noise (**Nodule Fusion(NF)**)
2. **for** each $NF \varepsilon NFs$ **do**
3. $NC \longleftarrow \Phi$ → Nodule Candidates
4. $VS \longleftarrow \Phi$ → Vessels
5. **if** Diameter$(l) < T_d^{(min)}$ then
6. **continue** → Noise
7. **end if**
8. **if** Volume $(l) > T_v^{(max)}$ or Overlapped $(l, VS) > T_0$ or $(Elongation\ (l) > T_e\ and\ Volume\ (l) > T_v^{(min)})$ **then**
9. $VS \longleftarrow VS \cup \{l\}$ → Vessels

10. **continue**
11. **end if**
12. **if** Diameter $(I) > T_a^{(max)}$ **then**
13. **continue** → Noise
14. **end if**
15. **if** Circularity $(I) > T_c$ and Area$(I) > T_a^{(min)}$ and Area$(I) < T_a^{(max)}$ **then**
16. $NC \longleftarrow NC \cup \{I\}$ → Nodule Candidates
17. **end if**
18. **end for**
19. **return NC**
20. **end function**

5.6 Classified Nodules:

Patient 1:

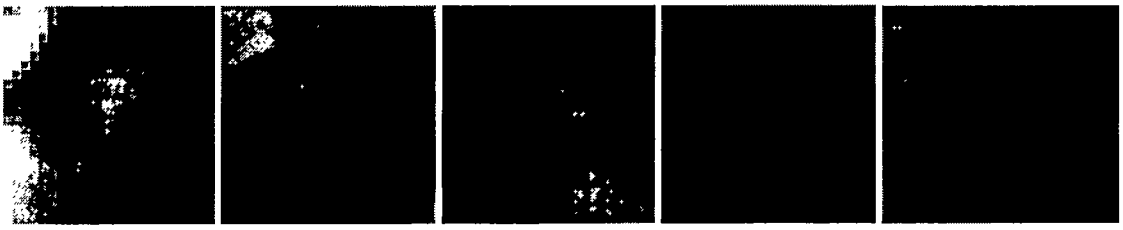

Patient 2:

Patient 3:

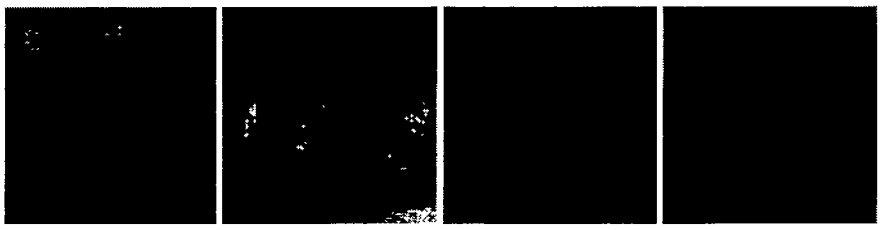

Patient 4:

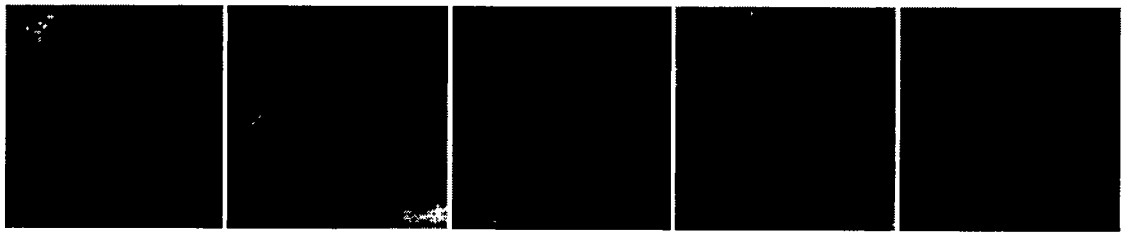

Patient 5:

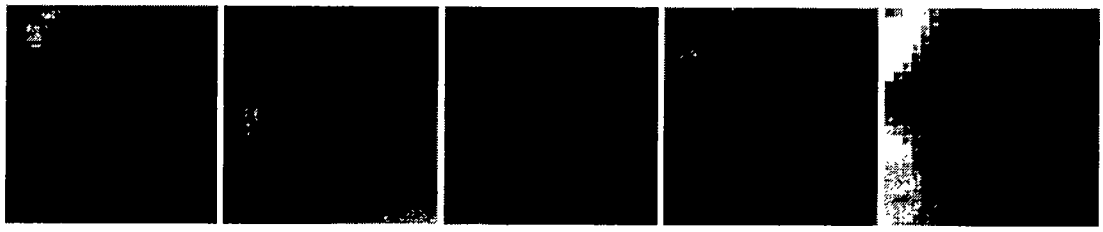

Patient 6:

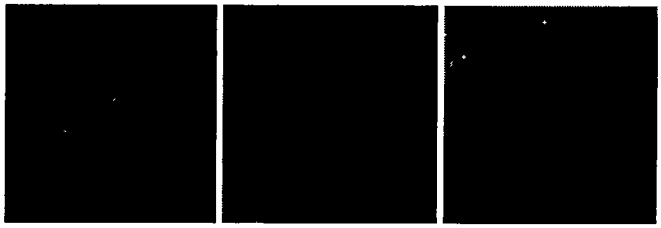

Patient 7:

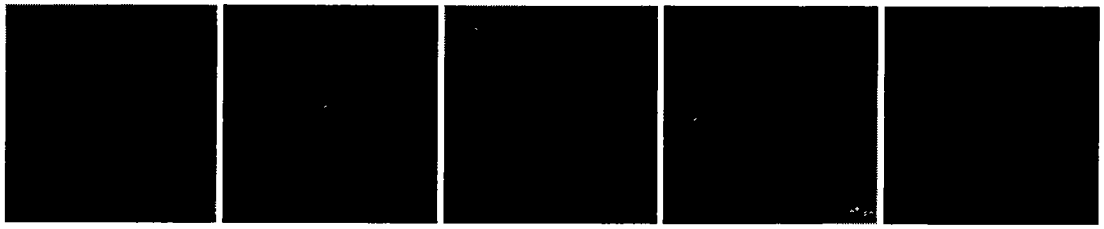

5.7 Comparison with other works:

CAD system	Nodule Size used(mm)	Average False Positives per case	Reported Sensitivity(%)/ Efficiency
Suzuki et al.	8-20	16.1	80.3
Rubin et al.	≥3	3	76
Opfer and Wiemeker	≥4	4	74
Messay et al.	3-30	3	82.66
Sahiner et al.	3-36.4	4.9	79
Wook Jin et al	3-30	5.45	94.1
Proposed CAD	3-30	4.85	95.2

5.8 Critical analysis:

In Wook Jin et al [80] proposed technique they focused on all three main types of nodules i.e. isolated nodules, juxtaplueral and juxtavescular nodules but due to complex structure of juxtavescular larger and non-solid nodules were not detected. We implement Wook Jin et al [80] technique and found that in thirteen images larger juxtavescular nodules were not detected in Wook Jin et al [80]. All these types of larger juxtavescular nodules and non-solid nodules were detected. In our work for larger juxtavescular nodules we used distance transform technique to detect larger juxtavescular nodules which were not detected in earlier techniques. Some example of those nodules is given below:

Wook Jin et al[80]:

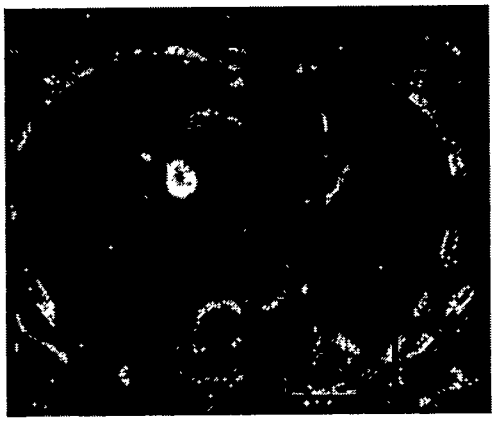

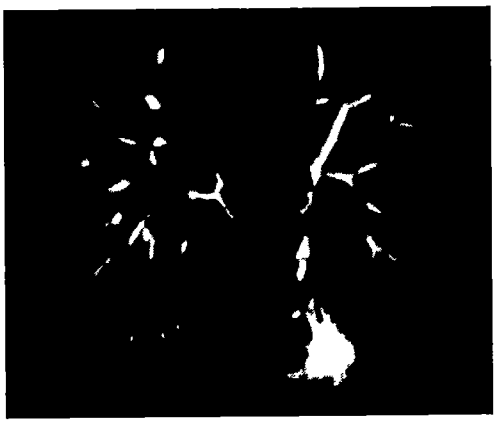

Proposed Technique:

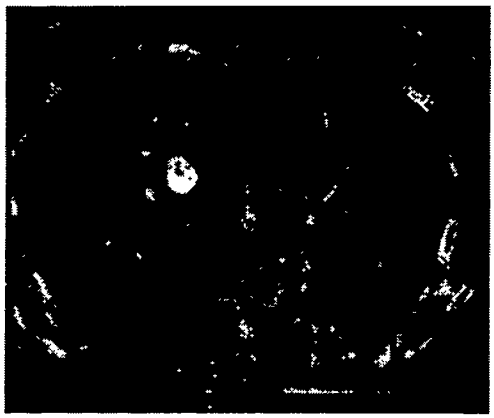

Segmentations

ROI

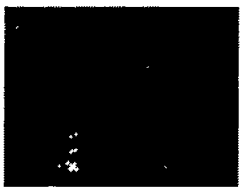

Detected Nodules

Chapter 6
Conclusion and Future Work

To detect nodule candidate from lungs without using a CAD system is a harder task for human beings so we developed this CAD scheme to help radiologist to detect lungs nodule and increase survival rate of lugs cancer's patients. In this CAD scheme firstly we segment the lungs by using Linear Interpolation and Lung Parenchymal Volume Identification then after it Region of Interest is extracted using multiple optimal thresholding then deformable model and distance transform applied to detect nodule candidates. False positives in our CAD scheme is 4.85 with high sensitivity level which is 95.2%. This CAD scheme is very helpful for radiologist and it is tested on LIDC databases.

In our work although we detected all kinds of nodules like isolated, juxtavescular and juxtaplueral nodules this work also required a second interpretation task which differentiate between benign and malignant lesions. Our work will help to categorize benign and malignant because all types of nodules are detected in this process the only task is remaining to categorize nodules in two different categories i.e. malignant and benign.

Chapter 7
References

References:

[1] A. Jemal, R. Siegel, E. Ward, Y. Hao, J. Xu, M.J. Thun, Cancer statistics, 2009, CA: A Cancer Journal for Clinicians 59 (2009) 225–249.

[2] K. Jung, Y. Won, S. Park, H. Kong, J. Sung, H. Shin, E. Park, J. Lee, Cancer statistics in Korea: incidence, mortality and survival in 2005, Journal of Korean Medical Science 24 (2009) 995–1003.

[3] Cancer research UK, \Cancer survival statistics for common cancers," http://www.cancerresearchuk.org/cancer-info/cancerstats/survival/commoncancers/.

[4] INCA Estimativas da Incidencia e Mortalidade por Cancer no Brasil, available in: http://www.inca.gov.br/estimativas/2003/versaofinal.pdf, 2003.

[5] D. J. Getty, R. M. Pickett, C. J. D'Orsi, and J. A. Swetts, "Enhanced interpretation of diagnostic images," Investigat. Radiol., vol. 23, pp.240–252, 1988.

[6] H. Chan, K. Doi, C. Vyborny, R. Schmidt, C. Metz, K. Lam, T. Orgura, Y. Wu, and H. MacMahon, "Improvement in radiolo- gists' detection of clustered micro calcifications on mammograms: The potential of computer-aided diagnosis," Investigat. Radiol.., vol. 2, pp.1102–1110, 1990.

[7] I. Sluimer, A. Schilham, M. Prokop, B. van Ginneken, Computer analysis of computer tomography scans of the lung: a survey, IEEE Transactions on Medical Imaging 25 (4)(2006) 385–405,doi:10.1109/TMI.2005.862753.

[8] Verisante, \The importance of early detection," http://www.verisante.com/cancer/other.

[9] Wook-Jin Choi and Tae-Sun Choi, \Automated pulmonary nodule detection system in computed tomography images: A hierarchical block classication approach," Entropy, vol. 15, no. 2, pp. 507{523, 2013.

[10] T Hara, M Hirose, X Zhou, H Fujita, T Kiryu, R Yokoyama, and H Hoshi, \Nodule detection in 3D chest CT images using 2nd order autocorrelation features," Engineering in Medicine and Biology Society, 2005. IEEE-EMBS 2005. 27th Annual International Conference of the, pp. 6247 { 6249, Dec 2005.

[11] B. Sahiner, H.-P. Chan, L.M. Hadjiiski, P.N. Cascade, E.A. Kazerooni, A.R. Chughtai,C. Poopat, T. Song, L. Frank, J. Stojanovska, A. Attili, Effect of CAD on Radiologists' detection of lung nodules on thoracic ct scans: analysis of an observer performance study by nodule size, Acad. Radiol.y 16 (12) (2009) 1518–1530, http://dx.doi.org/10.1016/j.acra.2009.08.006. (ISSN 1076-6332).

[12] R. Yuan, P.M. Vos, P.L. Cooperberg, Computer-aided detection in screening CT for pulmonary nodules, Am. J. Roentgenol. 186 (5) (2006) 1280–1287, http://dx.doi.org/10.2214/AJR.04.1969. URL/http://www.ajronline.org/cgi/content/abstract/186/5/1280S.

[13] K. Marten, C. Engelke, Computer-aided detection and automated CT volumetry of pulmonary nodules, Eur. Radiol. 17 (2007) 888–901, http://dx.doi.org/10.1007/s00330-006-0410-3, ISSN: 0938-7994.

[14] Q. Li, F. Li, K. Doi, Computerized detection of lung nodules in thin-section CT images by use of selective enhancement filters and an automated rule-based classifier, Acad.

Radiol. 15 (2) (2008) 165–175, http://dx.doi.org/10.1016/j.acra.2007.09.018, ISSN: 1076-6332.

[15] S. Matsuoka, Y. Kurihara, K. Yagihashi, H. Niimi, Y. Nakajima, Peripheral solitary pulmonary nodule: CT findings in patients with pulmonary emphysema1,Radiology 235 (1) (2005) 266–273, http://dx.doi.org/10.1148/radiol.2351040674. URL/http://radiology.rsna.org/content/235/1/266.abstractS.

[16] A. Khan, P.G. Herman, P. Vorwerk, P. Stevens, K.A. Rojas, M. Graver, Solitary pulmonary nodules: comparison of classification with standard, thin-section, and reference phantom CT, Radiology 179 (2) (1991) 477–481. URL/http://radiology.rsna.org/content/179/2/477.abstractS.

[17] N.F. Vittitoe, J.A. Baker, C.E. Floyd, Fractal texture analysis in computer-aided diagnosis of solitary pulmonary nodules, Acad. Radiol. 4 (2) (1997) 96–101, http://dx.doi.org/10.1016/S1076-6332(97)80005-0, ISSN: 1076-6332.

[18] K. Awai, K. Murao, A. Ozawa, M. Komi, H. Hayakawa, S. Hori, Y. Nishimura, Pulmonary nodules at chest CT: effect of computer-aided diagnosis on radiologists' detection performance, Radiology 230 (2) (2004) 347–352, http://dx.doi.org/10.1148/radiol.2302030049.
URL /http://radiology.rsna.org/content/230/2/347.abstractS

[19] Y.J. Jeong, C.A. Yi, K.S. Lee, Solitary pulmonary nodules: detection, characterization, and guidance for further diagnostic workup and treatment, Am. J. Roentgenol. 188 (1) (2007) 57–68, http://dx.doi.org/10.2214/AJR.05.2131.URL/http://www.ajronline.org/cgi/content/abstract/188/1/57S.

[20] Computer-aided diagnosis of small pulmonary nodules, Sem. Ultrasound CT MRI 21 (2) (2000) 116–128, ISSN 0887-2171, http://dx.doi.org.10.1016/S0887-2171(00)90018-0, the Solitary Pulmonary Nodule.

[21] M. Antonelli, G. Frosini, B. Lazzerini, F. Marcelloni, Automated detection of pulmonary nodules in CT scans, in: International Conference on Computational Intelligence for Modelling, Control and Automation, vol. 2, 2005, pp. 799–803 http://doi.ieeecomputersociety.org/101109CIMCA20051631566S.

[22] A.E.-B.G. Gimelfarb, R.F.M.A. El-Ghar, Computer aided characterization of the solitary pulmonary nodule using volumetric and contrast enhancement features, Acad. Rodiol. 12 (2005) 1310–1319.

[23] S. Ozekes, Rule based lung region segmentation and nodule detection via genetic algorithm trained template matching, Istanbul Commer. Univ. J. Sci. 6(11) (2007) 17–30.

[24] S. Ozekes, O. Osman, O.N. Ucan, Nodule detection in a lung region that's segmented with using genetic cellular neural networks and 3D template matching with fuzzy rule based thresholding, Korean J. Radiol. 9 (2008) 1–9.

[25] J. Pu, B. Zheng, J.K. Leader, X.-H. Wang, D. Gur, An automated CT based lung nodule detection scheme using geometric analysis of signed distance field, Med. Phys. 35 (8) (2008) 3453–3461. ISSN: 0094-2405.URL/http://www.biomedsearch.com/nih/automated-CT-based-lung-nodule/18777905.htmlS.

[26] C. Schneider, A. Amjadi, A. Richter, M. Fiebich, Automated lung nodule detection and segmentation, in: Proceeding of the SPIE, 72601T, vol. 7260,2009, http://dx.doi.org.10.1117/12.811985. URL /http://anode09.isi.uu.nl/results/Schn09.pdfS

[27] R. Opfer, R. Wiemker, Performance analysis for computer-aided lung nodule detection on LIDC data, in: Proceedings of the SPIE, vol. 6515, 2007, pp. 65151C–65151C-9. URL/http://link.aip.org/link/PSISDG/v6515/i1/p65151C/s1&Agg=doiS.

[28] Sua 'rez-Cuenca, W. Guo, Q. Li, Automated detection of pulmonary nodules in CT: false positive reduction by combining multiple classifiers, in: Proceedings of the SPIE, vol. 7963, 2011, pp. 796338–796338-6. URL/http://dx.doi.org/10.1117/12.878793S.

[29] C. Beigelman-Aubry, P. Raffy, W. Yang, R.A. Castellino, P.A.Grenier, Computer-aided detection of solid lung nodules on computer methods and programs in biomedicine 98 (2010)1–14 13 follow-up MDCT screening: evaluation of detection, tracking,and reading time, American Journal of Roentgenology 189 (4) (2007) 948–955, ISSN:1546–3141,doi:10.2214/AJR.07.2302.

[30] S.G. Armato, W.F. Sensakovic, Automated lung segmentation for thoracic CT: impact on computer-aided diagnosis,Academic Radiology 11 (2004) 1011–1021.

[31] I. Sluimer, A. Schilham, M. Prokop, B. van Ginneken, Computer analysis of computed tomography scans of the lung: a survey, IEEE Transactions on Medical Imaging 25 (4) (2006) 385–405,doi:10.1109/TMI.2005.862753.

[32] S. Hu, E.A. Hoffman, J.M. Reinhardt, Automatic lung segmentation for accurate quantitation of volumetric X-ray CT images, IEEE Transactions on Medical Imaging 20 (2001) 490–498.

[33] B. Zheng, J.K. L., G.S. Maitz, B.E. Chapman, C.R. Fuhrman, R.M. Rogers, F.C. Sciurba, A. Perez, P. Thompson, W.F. Good, D. Gur III, A simple method for automated lung segmentation in X-ray CT images, SPIE 5032 (2003)1455–1463,doi:10.1117/12.480290.

[34] J.K. Leader, B. Zheng, R.M. Rogers, F.C. Sciurba, A. Perez, B.E. Chapman, S. Patel, C.R. Fuhrman, D. Gur, Automated lung segmentation in X-ray computed tomography: development and evaluation of a heuristic threshold-based scheme, Academic Radiology 10 (11) (2003) 1224–1236.

[35] S.G. Armato, M.L. Giger, C.J. Moran, J.T. Blackburn, K. Doi, H. MacMahon, Computerized detection of pulmonary nodules on CT scans, Radiographics 19 (5) (1999) 1303–1311.

[36] J.P. Ko, M. Betke, C.T. Chest, Automated nodule detection and assessment of change over time—preliminary experience, Radiologic Clinics of North America 218 (2001)267–273.

[37] B. Zhao, D. Yankelevitz, Two-dimensional multi-criterion segmentation of pulmonary nodules on helical CT images,Medical Physics 26 (6) (1999) 889–895.

[38] B. Zhao, M.S. Ginsberg, R.A. Lefkowitz, L. Jiang, C. Cooper,L.H. Schwartz, Application of the LDM algorithm to identify small lung nodules on low-dose MSCT scans, SPIE 5370 (2004) 818–823,doi:10.1117/12.535558.

[39] T. Ezoe, H. Takizawa, S. Yamamoto, A. Shimizu, T. Matsumoto, Y. Tateno, T. Iimura, M. Matsumoto, Automatic detection method of lung cancers including ground-glass opacities from chest X-ray CT images, SPIE 4684 (2002) 1672–1680.

[40] C.I. Fetita, F. Preteux, C. Beigelman-Aubry, P. Grenier, 3D automated lung nodule segmentation in HRCT, Medical Image Computing and Computer-Assisted Intervention-MICCAI 2003 2878 (2003) 626–634.

[41] M. Tanino, H. Takizawa, S. Yamamoto, T. Matsumoto, Y. Tateno, T. Iinuma, A detection method of ground glass opacities in chest X-ray CT images using automatic clustering techniques, 1728–1737, 561–577, in: M. Sonka, J.M. Fitzpatrick (Eds.),

Society of Photo-Optical Instrumentation Engineers (SPIE) Conference Series, vol. 5032 of Presented at the Society of Photo-Optical Instrumentation Engineers (SPIE) Conference, 2003.

[42] K. Awai, K. Murao, A. Ozawa, M. Komi, H. Hayakawa, S. Hori,Y. Nishimura, Pulmonary nodules at chest CT: effect of computer-aided diagnosis on radiologists detection performance, Radiology 230 (2004) 347–352.

[43] K. Kanazawa, Y. Kawata, N. Niki, H. Satoh, H. Ohmatsu, R. Kakinuma, M. Kaneko, N. Moriyma, K. Eguchi,Computer-aided diagnosis for pulmonary nodules based on helical CT images, Computerized Medical Imaging and Graphics 22 (1998) 157–167.

[44] M.N. Gurcan, B. Sahiner, N. Petrick, H.P. Chan, E.A. Kazerooni, P.N. Cascade, L.M. Hadjiiski, Lung nodule detection on thoracic computed tomography images: preliminary evaluation of a computer-aided diagnosis system, Medical Physics (2002) 2552–2558.

[45] M. Kubo, K. Kubota, N. Yamada, Y. Kawata, N. Niki, K. Eguchi,H. Ohmatsu, R. Kakinuma, M. Kaneko, M. Kusumoto, K. Mori, H. Nishiyama, N. Moriyama, CAD system for lung cancer based on low-dose single-slice CT image, in: M. Sonka, J.M. Fitzpatrick (Eds.), Society of Photo-Optical Instrumentation Engineers (SPIE) Conference Series, vol. 4684 of Presented at he Society of Photo-Optical Instrumentation Engineers (SPIE) Conference, 2002, pp. 1262–1269.

[46] N. Yamada, M. Kubo, Y. Kawata, N. Niki, K. Eguchi, H. Omatsu, R. Kakinuma, M. Kaneko, M. Kusumoto, H.Nishiyama, N. Moriyama, ROI extraction of chest CT images using adaptive opening filter, in: M. Sonka, J.M. Fitzpatrick (Eds.), Society of Photo-Optical Instrumentation Engineers(SPIE) Conference Series, vol. 5032 of Presented at the Society of Photo-Optical Instrumentation Engineers (SPIE) Conference, 2003, pp. 869–876,doi:10.1117/12.483540.

[47] T. Oda, M. Kubo, Y. Kawata, N. Niki, K. Eguchi, H. Ohmatsu, R. Kakinuma, M. Kaneko, M. Kusumoto, N. Moriyama, K. Mori, H. Nishiyama, Detection algorithm of lung cancer candidate nodules on multislice CT images, in: M. Sonka, J.M. Fitzpatrick (Eds.), Society of Photo-Optical Instrumentation Engineers (SPIE) Conference Series, vol. 4684 of Presented at the Society of Photo-Optical Instrumentation Engineers (SPIE) Conference, 2002, pp. 1354–1361.

[48] S. Saita, T. Oda, M. Kubo, Y. Kawata, N. Niki, M. Sasagawa, H.Ohmatsu, R. Kakinuma, M. Kaneko, M. Kusumoto, K. Eguchi,H. Nishiyama, K. Mori, N. Moriyama, Nodule detection algorithm based on multislice CT images for lung cancer screening, in: J.M. Fitzpatrick, M. Sonka (Eds.), Society of Photo-Optical Instrumentation Engineers (SPIE) Conference Series, vol. 5370 of Presented at the Society of Photo-Optical Instrumentation Engineers (SPIE) Conference, 2004, pp.1083–1090,doi:10.1117/12.534826.

[49] R. Wiemker, P. Rogalla, A. Zwartkruis, T. Blaffert, Computer-aided lung nodule detection on high-resolution CT data, in: M. Sonka, J.M. Fitzpatrick (Eds.), Society of Photo-Optical Instrumentation Engineers (SPIE) Conference Series, vol. 4684 of Presented at the Society of Photo-Optical Instrumentation Engineers (SPIE) Conference, 2002, pp.677–688.

[50] S. Chang, H.D. Emoto, L.A. Metaxas, Pulmonary micronodule detection from 3-D chest CT, Lecture Notes in Computer Science-Medical Image Computing and Computer-Assisted Intervention 3217 (2004) 821–828.

[51] Q. Li, K. Doi, New selective nodule enhancement filter and its application for significant improvement of nodule detection on computed tomography, in: J.M. Fitzpatrick, M.Sonka (Eds.), Society of Photo-Optical Instrumentation Engineers (SPIE) Conference Series, vol. 5370 of Presented at the Society of Photo-Optical Instrumentation Engineers (SPIE) Conference, 2004, pp. 1–9,doi:10.1117/12.535802.

[52] D.S. Paik, Computer aided interpretation of medical images,Ph.D. Thesis, Stanford University, 2002.

[53] O. Osman, S. Ozekes, O.N. Ucan, Lung nodule diagnosis using 3D template matching, Computers in Biology and Medicine, 37 (8) (2007) 1167–1172, ISSN: 0010–4825, doi:10.1016/j.compbiomed.2006.10.007.

[54] A. Retico, P. Delogu, M.E. Fantacci, I. Gori, A. Preite Martinez, Lung nodule detection in low-dose and thin-slice computed tomography, Computers in Biology and Medicine, 38 (4)(2008) 525–534, ISSN: 0010–4825, doi:10.1016/j.compbiomed.2008.02.001.

[55] K.T. Bae, J.-S. Kim, Y.-H. Na, K.G. Kim, J.-H. Kim, Pulmonary nodules at chest CT: effect of computer-aided diagnosis on radiologists detection performance, Radiology 236 (2005) 286–293.

[56] Dolejsi, M., Kybic, J., Polovincak, M., Tuma, S., 2009. The Lung TIME: annotated lung nodule dataset and nodule detection framework, vol. 7260, SPIE, 72601U, doi: http://dx.doi.org/10.1117/12.811645, URL ⟨http://link.aip.org/link/?PSI/7260/72601U/1⟩.

[57] Dolejší, M., Kybic, J., 2008. Reducing false positive responses in lung nodule detector system by asymmetric AdaBoost. In: Proceedings of 2008 IEEE International Symposium on Biomedical Imaging: From Nano to Macro, IEEE,IEEE, 3 Park Avenue, 17th Floor, New York, NY 10016-5997, USA, pp. 656–659,ISBN 978-1-4244-2003-2.

[58] de Oliveira Campo, V., Feitosa, R.Q., Silva, A.C., Nunes, R.A., 2010. Multicriterion homogeneity metric for nodule segmentation and detection in computedtomography. In: Conci A. (Ed.), 17th International Conference onSystems, Signals and Image Processing (IWSSIP 2010), EdUFF, Rio de Janeiro, pp. 344–347

[59] Netto, S.M.B., Silva, A.C., Nunes, R.A., Gattass, M., 2012. Automatic segmentation of lung nodules with growing neural gas and support vector machine. Comput. Biol. Med. 42 (11), 1110–1121.

[60] Shiying Hu, Eric A. Hoffman, Joseph M. Reinhardt, Automatic lung segmentation for accurate quantitation of volumetric X-ray CT images, IEEE Trans. Med. Imag. 20 (6) (2001) 490–498.

[61] D.-Y. Kim, et al., Pulmonary nodule detection using chest CT images, Acta Radiol. 44 (3) (2003) 252–257.

[62] Jane P. Ko, Margrit Betke, Chest CT: automated nodule detection and assessment of change over time—preliminary experience, Radiology 218 (1) (2001)267–273.

[63] K. Suzuki, S.G. Armato III, F. Li, S. Sone, K. Doi, Massive training artificial neural network (MTANN) for reduction of false positives in computerized detection of lung nodules in low-dose computed tomography, Medical Physics 30 (2003) 1602–1617.

[64] A. Riccardi, T. Petkov, G. Ferri, M. Masotti, R. Campanini, Computer-aided detection of lung nodules via 3D fast radial transform, scale space representation, and Zernike MIP classification, Medical Physics 38 (2011) 1962–1971.

[65] D. Cascio, R. Magro, F. Fauci, M. Iacomi, G. Raso, Automatic detection of lung nodules in CT datasets based on stable 3D mass-pring models, Computers in Biology and Medicine 42(2012) 1098–1109.

[66] R. Pohle, K. D. Toennies, "Segmentation of Medical Images Using Adaptive Region Growing", Department of Simulation and Graphics,Otto-von-Guericke University Magdeburg, 2001

[67] Swati p. Tidke, Vrishali A, Chakkarwar, "Classification of lung tumor using SVM", International Journal of computational Engineering Research, 2012, Vol.2, issue 5, pp.1254-1257.

[68] Bastawrous, H.A.Fukumoto, T. ; Tsudagawa, M. ; Nitta, N, "Detection of Ground Glass Opacities in Lung CT Images Using Gabor Filters and Neural Networks", Instrumentation and Measurement Technology Conference, 2005, Proceedings of the IEEE ,vol. 1, pp. 251 – 256.

[69] Dehmeshki J, Ye X, Casique MV, Lin X. A hybrid approach for automated detection of lung nodules in CT images. In: Kovacevic E, Meijering J, editors. IEEE international symposium on biomedical imaging: nano to macro, 2006. 3rd. Institute of Electrical and Electronics Engineers; 2006. p. 506–9.

[70] J.a.R.F. da Silva Sousa, A.C. Silva, A.C. de Paiva, R.A. Nunes, Methodology for automatic detection of lung nodules in computerized tomography images, Comput. Methods Prog.Biomed. 98 (1) (2010) 1–14, http://dx.doi.org/10.1016/j.cmpb.2009.07.006, ISSN: 0169-2607.

[71] X. Ye, G. Beddoe, G. Slabaugh, Graph cut-based automatic segmentation of lung nodules using shape, intensity, and spatial features, in: The Second International Workshop on Pulmonary Image Analysis, 2009, pp. 103–113.

[72] Opfer R, Wiemker R. Medical imaging 2007: image perception, observer performance, and technology assessment. San Diego, CA. In: Society ofPhotoOptical Instrumentation Engineers (SPIE) conference series, vol. 6515, SPIE proceedings. 2007., http://dx.doi.org/10.1117/12.708210.

[73] Nie S-D, Chen Z-X, Li L-H. A CI feature-based pulmonary nodule segmentation using three-domain mean shift clustering. In: Tang YY, editor. IEEE international conference on wavelet analysis and pattern recognition, 2007. ICWAPR'07, vol. 1. Institute of Electrical and Electronics Engineers; 2007. p.223–7, http://dx.doi.org/10.1109/ICWAPR.2007.4420699.

[74] T. Messay, R. Hardie, S. Rogers, A new computationally efficient CAD system for pulmonary nodule detection in CT imagery, Medical Image Analysis 14 (2010) 390–406.

[75] Xiaomin P, Hongyu G, Jianping D. Computerized detection of lung nodules in CT images by use of multiscale filters and geometrical constraint region growing. In: Lu W, Sun L, Zhang X, Sun J, editors. 2010 4th international conference on bioinformatics and biomedical engineering (iCBBE). Institute of Electrical and

Electronics Engineers; 2010. p. 1–4, http://dx.doi.org/10.1109/ICBBE.2010.5517771. ISSN 2151-7614.

[76] Tan M, Deklerck R, Jansen B, Bister M, Cornelis J. A novel computer-aided lung nodule detection system for CT images. Medical Physics 2011;38(10):5630–45, http://dx.doi.org/10.1118/1.3633941.

[77] S. Lee, A. Kouzani, E. Hu, Automated identification of lung nodules, in: 2008 IEEE Tenth Workshop on Multimedia Signal Processing, 2008, pp. 497–502, http://dx.doi.org.10.1109/MMSP.2008.4665129.

[78] N. Camarlinghi, I. Gori, A. Retico, R. Bellotti, P.Bosco, P. Cerello, G. Gargano, E. Lopez Torres, R. Megna, M. Peccarisi, M. Fantacci, Combination of computer-aided detection algorithms for automatic lung nodule identification, Int. J. Comput. Assisted Radiol. Surg. (2011) 1–10, ISSN: 1861-6410, URL http://dx.doi.org.10.1007/s11548-011-0637-6.

[79] Chama CK, Mukhopadhyay S, Biswas PK, Dhara AK, Madaiah MK, KhandelwalN. Automated lung field segmentation in CT images using mean shift clustering and geometrical features; 2013, http://dx.doi.org/10.1117/12.2007910.

[80] W. Choi, T. Choi, Genetic programming-based feature transform and classification for the automatic detection of pulmonary nodules on computed tomography images, Information Sciences 212 (2012) 57–78.

[81] D. Cascio, R. Magro, F. Fauci M, Iacomi, G. Raso Automatic detection of lung nodules in CT datasets based on stable 3D mass–spring models Dipartimento di Fisica, Universit!a degli Studi di Palermo, Italy Institutul de S- tiint¸e Spat¸iale, P.O. Box MG-23, Ro 077125, Bucharest-M˜agurele, Romania.

so to include those larger juxtavescular nodules we apply distance transform using 3D region growing algorithm. We used seed points which were identified in section **3.4.** As a matter of first importance the structures are regrouped by utilizing 3D district developing calculation to section structure which are joined with one another. The resultant structures are not partitioned into genuine structures (knobs, vessels and bronchi) as of right now.

Presently to get the genuine knobs hopeful, we here connected separation change. State of the knobs is most imperative element which is utilized to partitioned it from different structures. Separation change give every one of us essential data about shape, by utilizing this data it is anything but difficult to particular round shapes (more probable knobs) from barrel shaped shapes (more probable vessels).Distance change is figured [18] in each of the structures begins from one quality in all voxels of the edges and as we moved to the inward voxel it is increased, until there is one and only or two voxels left at the same separation from the edge. Tubular and extended structures have consistent estimations of the separation change with little interims along their more noteworthy length. Structures with expansive grouping of knobs have a high estimation of the separation change. This expansive worth highlights the circular way of the lung knob, so division of bigger juxtavescular knobs from alternate structures, for example, vessel and bronchi and so on., is finished by investigating the round and hollow component of the vessel and bronchi.

4.5.3 Nodules Fusion:

After detection of all the types of nodule candidates at this stage we have to merge all those types of nodules before performing rule based pruning. So we take union of all the detected nodules to avoid the duplication and to make the rule based pruning much easier.

4.5.4 False positive reduction using rule based pruning:

Nodule candidate detected at the pervious stage may include some non-nodule candidates, so to remove those candidates and to ensure accuracy of our detected rules here we perform rule based pruning. In other words to reduce false positives we perform rule based pruning.